N-1857

April 1993

By Erick T. Huang

Sponsored By
Chief of Naval Research

# NCEL
## Technical Note

# NONLINEAR WAVE FORCES ON LARGE OCEAN STRUCTURES



***ABSTRACT*** This study explores the significance of second-order wave excitations on a large pontoon and tests the feasibility of reducing a nonlinear free surface problem by perturbation expansions. A simulation model has been developed based on the perturbation expansion technique to estimate the wave forces. The model uses a versatile finite element procedure for the solution of the reduced linear boundary value problems. This procedure achieves a fair compromise between computation costs and physical details by using a combination of 2D and 3D elements. A simple hydraulic model test was conducted to observe the wave forces imposed on a rectangle box by Cnoidal waves in shallow water. The test measurements are consistent with the numerical predictions by the simulation model. This result shows favorable support to the perturbation approach for estimating the nonlinear wave forces on shallow draft vessels. However, more sophisticated model tests are required for a full justification. Both theoretical and experimental results show profound second-order forces that could substantially impact the design of ocean facilities.



NAVAL CIVIL ENGINEERING LABORATORY PORT HUENEME CALIFORNIA 93043-5003

# METRIC CONVERSION FACTORS

## Approximate Conversions to Metric Measures

| Symbol | When You Know | Multiply by | To Find | Symbol |
|---|---|---|---|---|
| | | **LENGTH** | | |
| in | inches | *2.5 | centimeters | cm |
| ft | feet | 30 | centimeters | cm |
| yd | yards | 0.9 | meters | m |
| mi | miles | 1.6 | kilometers | km |
| | | **AREA** | | |
| $in^2$ | square inches | 6.5 | square centimeters | $cm^2$ |
| $ft^2$ | square feet | 0.09 | square meters | $m^2$ |
| $yd^2$ | square yards | 0.8 | square meters | $m^2$ |
| $mi^2$ | square miles | 2.6 | square kilometers | $km^2$ |
| | acres | 0.4 | hectares | ha |
| | | **MASS (weight)** | | |
| oz | ounces | 28 | grams | g |
| lb | pounds | 0.45 | kilograms | kg |
| | short tons (2,000 lb) | 0.9 | tonnes | t |
| | | **VOLUME** | | |
| tsp | teaspoons | 5 | milliliters | ml |
| Tbsp | tablespoons | 15 | milliliters | ml |
| fl oz | fluid ounces | 30 | milliliters | ml |
| c | cups | 0.24 | liters | l |
| pt | pints | 0.47 | liters | l |
| qt | quarts | 0.95 | liters | l |
| gal | gallons | 3.8 | liters | l |
| $ft^3$ | cubic feet | 0.03 | cubic meters | $m^3$ |
| $yd^3$ | cubic yards | 0.76 | cubic meters | $m^3$ |
| | | **TEMPERATURE (exact)** | | |
| °F | Fahrenheit temperature | 5/9 (after subtracting 32) | Celsius temperature | °C |

*1 in = 2.54 (exactly). For other exact conversions and more detailed tables, see NBS Misc. Publ. 286, Units of Weights and Measures, Price $2.25, SD Catalog No. C13.10:286.

## Approximate Conversions from Metric Measures

| Symbol | When You Know | Multiply by | To Find | Symbol |
|---|---|---|---|---|
| | | **LENGTH** | | |
| mm | millimeters | 0.04 | inches | in |
| cm | centimeters | 0.4 | inches | in |
| m | meters | 3.3 | feet | ft |
| m | meters | 1.1 | yards | yd |
| km | kilometers | 0.6 | miles | mi |
| | | **AREA** | | |
| $cm^2$ | square centimeters | 0.16 | square inches | $in^2$ |
| $m^2$ | square meters | 1.2 | square yards | $yd^2$ |
| $km^2$ | square kilometers | 0.4 | square miles | $mi^2$ |
| ha | hectares (10,000 $m^2$) | 2.5 | acres | |
| | | **MASS (weight)** | | |
| g | grams | 0.035 | ounces | oz |
| kg | kilograms | 2.2 | pounds | lb |
| t | tonnes (1,000 kg) | 1.1 | short tons | |
| | | **VOLUME** | | |
| ml | milliliters | 0.03 | fluid ounces | fl oz |
| l | liters | 2.1 | pints | pt |
| l | liters | 1.06 | quarts | qt |
| l | liters | 0.26 | gallons | gal |
| $m^3$ | cubic meters | 35 | cubic feet | $ft^3$ |
| $m^3$ | cubic meters | 1.3 | cubic yards | $yd^3$ |
| | | **TEMPERATURE (exact)** | | |
| °C | Celsius temperature | 9/5 (then add 32) | Fahrenheit temperature | °F |

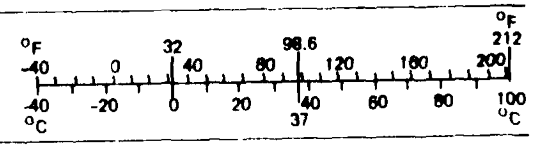

| REPORT DOCUMENTATION PAGE | Form Approved OMB No. 0704-018 |
|---|---|



**1. AGENCY USE ONLY** *(Leave blank)*

**2. REPORT DATE**
April 1993

**3. REPORT TYPE AND DATES COVERED**
Final: Oct 1991 through Sep 1992

**4. TITLE AND SUBTITLE**
NONLINEAR WAVE FORCES ON LARGE OCEAN STRUCTURES

**5. FUNDING NUMBERS**
PR - R000-N0-210
WU - DN661001

**6. AUTHOR(S)**
Erick T. Huang

**7. PERFORMING ORGANIZATION NAME(S) AND ADDRESSE(S)**
Naval Civil Engineering Laboratory
Port Hueneme, CA 93043-4328

**8. PERFORMING ORGANIZATION REPORT NUMBER**
TN - 1857

**9. SPONSORING/MONITORING AGENCY NAME(S) AND ADDRESSE(S)**
Chief of Naval Research
Office of NavalResearch
Arlington, VA 22217-5000

**10. SPONSORING/MONITORING AGENCY REPORT NUMBER**

**11. SUPPLEMENTARY NOTES**

**12a. DISTRIBUTION/AVAILABILITY STATEMENT**
Approved for public release; distribution unlimited.

**12b. DISTRIBUTION CODE**

**13. ABSTRACT** *(Maximum 200 words)*

This study explores the significance of second-order wave excitations on a large pontoon and tests the feasibility of reducing a nonlinear free surface problem by perturbation expansions. A simulation model has been developed based on the perturbation expansion technique to estimate the wave forces. The model uses a versatile finite element procedure for the solution of the reduced linear boundary value problems. This procedure achieves a fair compromise between computation costs and physical details by using a combination of 2D and 3D elements. A simple hydraulic model test was conducted to observe the wave forces imposed on a rectangle box by Cnoidal waves in shallow water. The test measurements are consistent with the numerical predictions by the simulation model. This result shows favorable support to the perturbation approach for estimating the nonlinear wave forces on shallow draft vessels. However, more sophisticated model tests are required for a full justification. Both theoretical and experimental results show profound second-order forces that could substantially impact the design of ocean facilities.

**14. SUBJECT TERMS**
Nonlinear wave forces, perturbation expansion, finite element method, large floating bodies

**15. NUMBER OF PAGES**
56

**16. PRICE CODE**

| 17. SECURITY CLASSIFICATION OF REPORT | 18. SECURITY CLASSIFICATION OF THIS PAGE | 19. SECURITY CLASSIFICATION OF ABSTRACT | 20. LIMITATION OF ABSTRACT |
|---|---|---|---|
| Unclassified | Unclassified | Unclassified | UL |

CONTENTS

## INTRODUCTION

Existing analytical models for the prediction of wave excitation of ocean structures assume that the amplitudes of waves and structure motions are small in comparison with the wavelength and the nominal dimension of structures. Thus, the diffraction waves from the structure may be approximated by a simple harmonic function. These assumptions preclude their application in severe sea states. Large waves, in fact, present a much steeper profile than that of a simple harmonic function. A precise description of the wave kinematics requires retention and proper treatment of higher order terms of the equation of motion and a proper specification of the water body boundary at the free surface. These two factors, which are ignored in linearized approximations, are the principle sources of wave nonlinearity. When these nonlinear effects are included in the diffraction of waves by a body there are, at second order, interactions at the sums and differences of the component frequencies of the incident waves. Although the magnitudes of these nonlinear effects are, in general, only second order, they act at frequencies away from that of the ambient wave energy, and may therefore be of primary concern. This is especially true when these excitations are near the natural periods of the body motions or where restoring or damping forces are small. With the presence of large waves, second-order effects are important corrections to the linearized results.

Theoretical developments of the second-order diffraction problem have until recently been limited. Studies on simple geometry of the uniform vertical circular cylinder were conducted by Issacson (Ref 1), Chakrabarti (Ref 2), Molin (Ref 3), Wehausen (Ref 4), Hunt and Baddour (Ref 5), Chen and Hudspeth (Ref 6), Rahman (Ref 7), and Ogilvie (Ref 8). The results are, however, controversial due to the difficulties in the correct treatment of the second-order free surface boundary condition and a proper specification of the radiation condition for the second-order diffracted waves. Previous studies indicate that a weakly nonlinear diffraction problem may be reduced to a set of linear boundary problems by the perturbation method. Solutions may be obtained by Green's function method or the finite element method. Kim and Yue (Ref 9) presented a second-order diffraction solution for an axisymmetric body in constant water depth following the former approach. The solution gives an explicit second-order flow potential in terms of wave-source Green functions. The nonlinear forces, accurate to the second order, include slowly varying drift forces and biharmonic forces, which appear at a frequency twice that of the incident wave. The present study pursues the finite element method approach, which gives the possibility of addressing a sloping sea bottom of irregular geometry.

An immediate need for these analytical techniques exists at the Naval Civil Engineering Laboratory (NCEL) in the design of connectors for a pontoon-supported waterfront facility. The requirement of including a second-order diffraction force in the assessment of extreme environmental forces imposed by maximum design waves is an apparent trend in the near future.

## PROBLEM DEFINITION

A mathematical idealization of hydrodynamic couplings between waves and a group of large floating or fixed structures in water with a free surface is defined in Figure 1. Wave activity around the structures, hydrodynamic loads on the structures, and the resulting motion of the structure are investigated. The water body may be open or partially sheltered, and the water depth may vary. Relevant waves, including incident, scattering, and radiation waves, are described in a way similar to Stokes' second-order theory. The water body is divided into a three-dimensional (3D) region $\Omega_1$, and a two-dimensional (2D) region $\Omega_2$. The 3D region includes areas near structures where the seafloor may change substantially and the 2D region includes the remaining areas where the seafloor is reasonably flat. In 3D regions, waves are addressed in detail in 3D space to account for the effects due to irregular geometries of structures and the seafloor. In 2D regions, waves are approximated by plane wave theories (Ref 10) in terms of free surface parameters for better computation efficiency. Boundaries of these two regions are illustrated in Figure 1. These boundaries are the radiation boundary, $\Gamma_2$, which truncates the water domain to a finite area, and the border separating the two regions, $\Gamma_1$. Waves transmitted beyond the radiation boundary are accounted for in a collective form in terms of parameters on the radiation boundary. Incident waves are specified on the wave input boundary $\Gamma_I$, which coincides with the radiation boundary for convenience, when wind wave excitations are considered. Other boundaries involved are the sea bottom, $\Gamma_b$, the wetted surfaces of floating structures, $\Gamma_s$, and fixed structures, $\Gamma_w$. Subdivisions of the water body and the associated boundaries are illustrated in Figure 2.

## PROBLEM FORMULATION

A Cartesian coordinate system (OXYZ) fixed to the earth, as shown in Figure 3, is employed as an inertia reference, where the X-Y plane lies on the mean water surface and the Z coordinate is measured positive upward from the still water. The responses of a floating body are described in reference to a body coordinate system, Gxyz, attached to the body, with its origin G located at the center of gravity of the body. The xy plane is parallel to the static waterplane and the z coordinate is directed vertically upward. For the purpose of computing wave drift forces and moments exerted on the body, a third system of coordinate axes $(G\hat{x}\hat{y}\hat{z})$ is defined where its origin is at the center of gravity of the body and is always parallel to the fixed coordinate system OXYZ.

With the assumption that the fluid is inviscid and incompressible and that the flow is irrotational, the relevant wave problems can be addressed using potential flow theory.

Assuming weakly nonlinear waves, the total velocity potential $\Phi$ is expressed as a perturbation in the wave slope parameter $\epsilon \equiv kA < 1$:

$$\Phi = \varepsilon \Phi^{(1)} + \varepsilon^2 \Phi^{(2)} + 0(\varepsilon^3) \tag{1}$$

where:

$\Phi^{(1)}$ = first-order velocity potential

$\Phi^{(2)}$ = second-order velocity potential

Further, k is the incident wave number given by the dispersion relationship $\omega^2 = gk \tanh(kh)$, and g is the gravitational acceleration. The associated free surface profile $\eta$ is decomposed likewise:

$$\eta = \epsilon\eta^{(1)} + \epsilon^2\eta^{(2)} + O(\epsilon^3)$$

This approximation leads to the decomposition of the otherwise nonlinear boundary value problem to a set of two linear boundary value problems. The first order problem has been described in Reference 11. This discussion will be limited to the second order.

The first- and second-order potentials must comply with the Laplace equation and appropriate boundary conditions as follows.

**First-Order Boundary Value Problem**

Laplace equation (fluid domain): $\nabla^2 \Phi^{(1)} = 0$ (2)

Seabed and fixed structure boundary: $\dfrac{\partial \Phi^{(1)}}{\partial n} = 0$ (3)

Floating structure boundary: $\dfrac{\partial \Phi^{(1)}}{\partial n} = v_n$ (4)

Free surface: $g\,\Phi_z^{(1)} + \Phi_{tt}^{(1)} = 0$ (5)

Radiation condition: $\lim\limits_{R\to\infty} \sqrt{R}\left(\dfrac{\partial}{\partial R}\,\phi^{(1)} - i\,k\,\phi^{(1)}\right) = 0$ (6)

**Second-Order Boundary Value Problem**

Laplace equation (fluid domain): $\nabla^2 \Phi^{(2)} = 0$ (7)

Seabed and fixed structure boundary: $\dfrac{\partial \Phi^{(2)}}{\partial n} = 0$ (8)

Floating structure boundary:

For radiation waves: $\frac{\partial \Phi^{(2)}}{\partial \mathbf{n}} = v_n$ (9)

For scattered and incident waves:

$$\frac{\partial \Phi^{(2)}}{\partial \mathbf{n}} = -(\mathbf{x}^{(1)} \cdot \nabla) \nabla \Phi^{(1)} \cdot \mathbf{n} + (\mathbf{v}^{(1)} - \nabla \Phi^{(1)}) \cdot \mathbf{N}^{(1)} \text{ at body surface.} \tag{10}$$

Free surface:

$$\Phi^{(2)}_{tt} + g\,\Phi^{(2)}_{z} = -2\,\nabla \Phi^{(1)} \cdot \nabla \Phi^{(1)}_{t} + \Phi^{(1)}_{t}\left(\Phi^{(1)}_{zz} + \frac{1}{g}\,\Phi^{(1)}_{ttz}\right) \text{ on } Z = 0. \tag{11}$$

Radiation condition: outgoing waves from the floating bodies.

In the above, $R = (x^2 + y^2)^{1/2}$ is the radial distance from the origin of the inertia frame, and $\frac{\partial}{\partial \mathbf{n}}$ is the normal derivative into the body. The second-order problem is complicated by the inhomogeneous forcing term in the free surface boundary condition (Equation 10), which is given in terms of quadratic products of the first-order potential. The first-order problem is classical and a variety of numerical solutions are available. For example, a solution using a finite element scheme has been obtained in a previous study (Ref 11). Equations 10 and 11 correlate $\Phi^{(2)}$ with $\Phi^{(1)}$. Hence, $\Phi^{(2)}$ is completely defined once $\Phi^{(1)}$ is known.

The first-order velocity potential may be expressed in component waves as follows.:

$$\Phi^{(1)} = \Phi^{(1)}_{I} + \Phi^{(1)}_{S} + \Phi^{(1)}_{B} \tag{12}$$

where:

$\Phi^{(1)}_{I}$ = first order incident wave potential

$\Phi^{(1)}_{S}$ = first order diffraction wave potential

$\Phi^{(1)}_{B}$ = first order radiation wave potential

For monochromatic incident waves, the time dependency is separated and rewritten:

$$\Phi^{(1)} = \left[\phi^{(1)}_{I} + \phi^{(1)}_{S} + \phi^{(1)}_{B}\right] e^{-i\omega t} \tag{13}$$

Substituting Equation 13 into the second-order free surface boundary condition in Equation 11, a quadratic periodic forcing function is obtained which oscillates at twice the frequency of the linear waves. As a result, Equation 11 may be written as:

$$\Phi^{(2)}_{tt} + g\,\Phi^{(2)}_{Z} = Q(x,y,0)\,e^{-2i\omega t} \tag{14}$$

where the quadratic forcing function Q(x,y,0) consists of nine components as follows:

$$Q(x,y,0) = Q_{II} + Q_{SS} + Q_{BB} + (Q_{IS} + Q_{SI}) + (Q_{IB} + Q_{BI}) + (Q_{SB} + Q_{BS}) \tag{15}$$

where:

$Q_{II}$ = plane wave forcing function which leads to the ordinary Stokes' second-order wave component at double frequency $2\omega$

$Q_{SS}$, $Q_{BB}$ = self interactions of first-order scattered waves and first-order radiation waves, respectively

$Q_{IS}, \ldots, Q_{BS}$ = cross interaction of the first-order terms

The details of these components are given in the following:

$$Q_{II} = i\,\omega\left[2(\nabla\phi^{(1)}_{I})^2 - \phi^{(1)}_{I}\,\phi^{(1)}_{IZZ} + \frac{\omega^2}{g}\,\phi^{(1)}_{I}\,\phi^{(1)}_{IZ}\right]$$

$$Q_{SS} = i\,\omega\left[2(\nabla\phi^{(1)}_{S})^2 - \phi^{(1)}_{S}\,\phi^{(1)}_{SZZ} + \frac{\omega^2}{g}\,\phi^{(1)}_{S}\,\phi^{(1)}_{SZ}\right]$$

$$Q_{BB} = i\,\omega\left[2(\nabla\phi^{(1)}_{B})^2 - \phi^{(1)}_{B}\,\phi^{(1)}_{BZZ} + \frac{\omega^2}{g}\,\phi^{(1)}_{B}\,\phi^{(1)}_{BZ}\right]$$

$$Q_{IS} = i\,\omega\left[2(\nabla\phi^{(1)}_{I})(\nabla\phi^{(1)}_{S}) - \phi^{(1)}_{I}\,\phi^{(1)}_{SZZ} + \frac{\omega^2}{g}\,\phi^{(1)}_{I}\,\phi^{(1)}_{SZ}\right]$$

$$Q_{SI} = i\omega\left[2(\nabla\phi_S^{(1)})(\nabla\phi_I^{(1)}) - \phi_S^{(1)}\phi_{IZZ}^{(1)} + \frac{\omega^2}{g}\phi_S^{(1)}\phi_{IZ}^{(1)}\right] \tag{16}$$

$$Q_{IB} = i\omega\left[2(\nabla\phi_I^{(1)})(\nabla\phi_B^{(1)}) - \phi_I^{(1)}\phi_{BZZ}^{(1)} + \frac{\omega^2}{g}\phi_I^{(1)}\phi_{BZ}^{(1)}\right]$$

$$Q_{BI} = i\omega\left[2(\nabla\phi_B^{(1)})(\nabla\phi_I^{(1)}) - \phi_B^{(1)}\phi_{IZZ}^{(1)} + \frac{\omega^2}{g}\phi_B^{(1)}\phi_{IZ}^{(1)}\right]$$

$$Q_{SB} = i\omega\left[2(\nabla\phi_S^{(1)})(\nabla\phi_B^{(1)}) - \phi_S^{(1)}\phi_{BZZ}^{(1)} + \frac{\omega^2}{g}\phi_S^{(1)}\phi_{BZ}^{(1)}\right]$$

$$Q_{BS} = i\omega\left[2(\nabla\phi_B^{(1)})(\nabla\phi_S^{(1)}) - \phi_B^{(1)}\phi_{SZZ}^{(1)} + \frac{\omega^2}{g}\phi_B^{(1)}\phi_{SZ}^{(1)}\right]$$

where the subscriptions of spatial coordinates indicate partial differential. These quadratic forcing function terms behave like a nonuniform pressure field applied to the free surface in first-order problems as described by Wehausen and Laitone (Ref 12). They generate additional cylindrical standing and outwardly going progressive waves at the double frequency.

Since Equation 14 is nonhomogeneous, the second-order potential consists of the homogeneous solution $\Phi^{(2)H}$ and the particular solution $\Phi^{(2)P}$ as:

$$\begin{aligned} \Phi^{(2)} &= \Phi^{(2)P} + \Phi^{(2)H} \\ &= \left(\phi^{(2)P} + \phi^{(2)H}\right)e^{-i2\omega t} \end{aligned} \tag{17}$$

These components satisfy, respectively, the homogeneous and inhomogeneous force surface condition (Equation 11), and jointly, the inhomogeneous body boundary condition, Equation 9 or 10. The particular solution may be further separated as:

$$\begin{aligned} \Phi^{(2)P} = {} & \Phi_{II}^{(2)} + \Phi_{SS}^{(2)} + \Phi_{BB}^{(2)} + (\Phi_{IS}^{(2)} + \Phi_{SI}^{(2)}) \\ & + (\Phi_{IB}^{(2)} + \Phi_{BI}^{(2)}) + (\Phi_{BS}^{(2)} + \Phi_{SB}^{(2)}) \end{aligned} \tag{18}$$

The homogeneous solution consists of:

$$\Phi^{(2)H} = \Phi_S^{(2)} + \Phi_B^{(2)} \tag{19}$$

By substituting Equations 18 and 19 into Equation 17, the total second-order potential becomes:

$$\Phi^{(2)} = \Phi_{II}^{(2)} + \left[\Phi_{SS}^{(2)} + \Phi_{BB}^{(2)} + (\Phi_{IS}^{(2)} + \Phi_{SI}^{(2)}) + (\Phi_{IB}^{(2)} + \Phi_{BI}^{(2)}) + (\Phi_{BS}^{(2)} + \Phi_{SB}^{(2)})\right] + \Phi_S^{(2)} + \Phi_B^{(2)} \tag{20}$$

or

$$\Phi^{(2)} = \Phi_{II}^{(2)} + \Phi_{D+S}^{(2)} + \Phi_B^{(2)} \tag{21}$$

where:

$$\Phi_{D+S}^{(2)} = \left[\Phi_{SS}^{(2)} + \Phi_{BB}^{(2)} + (\Phi_{IS}^{(2)} + \Phi_{SI}^{(2)}) + (\Phi_{IB}^{(2)} + \Phi_{BI}^{(2)}) + (\Phi_{BS}^{(2)} + \Phi_{SB}^{(2)})\right] + \Phi_S^{(2)}$$

The component $\Phi_{II}^{(2)}$ represents the forced wave motion generated by the $Q_{II}$ forcing function, which is the usual second-order Stokes' wave. $\Phi_S^{(2)}$ is the second-order scattered wave potential and $\Phi_B^{(2)}$ is the second order radiation wave potential generated by body motion. Both satisfy the homogeneous free surface boundary condition. Their far field behavior is given by:

$$\Phi_H \sim r^{-\frac{1}{2}} e^{ik_2 r} + 0\,(r^{-\frac{3}{2}}),\; r > 1$$

where $k_2$ is the double frequency wave number satisfying $4\omega^2 = gk_2 \tanh(kh)$. This means that, in principle, these components can be solved by the existing first-order method.

The second-order potential $\Phi^{(2)}$ in Equation 21 consists of three parts: (1) the incident wave component $\Phi_{II}^{(2)}$, (2) the pseudo-diffraction $\Phi_{D+S}^{(2)}$, and (3) the radiation components $\Phi_B^{(2)}$. The second-order incident wave potential is given by:

$$\Phi_{II}^{(2)} = \frac{3}{8}\,\frac{\pi H}{k T}\left(\frac{\pi H}{L}\right)\frac{\cosh[2k(d+z)]}{\sinh^4(kd)}\,e^{-i2\omega t} \qquad (22)$$

The radiation components satisfy the same equations as the radiation potentials of the first-order potential theory, at the double frequency $2\omega$. Newton's law applies through the use of Bernoulli's equation in the computation of the second-order wave exciting loads, which results in the equations of motion at the second ord~r, to be discussed later.

The solution procedure for Equation 14 using finite element method is straightforward, regardless of the complexity of the forcing function on the right-hand side of the equation.

## FINITE ELEMENT FORMULATIONS

According to the calculus of variations (Ref 13), the solution to a boundary value problem is the potential which minimizes a certain functional, in terms of the governing equation of the problem. For $\Phi^{(2)}$, the functional $\Pi^{(2)}$ can be expressed as:

$$\Pi^{(2)} = \iiint_{\Omega} \frac{1}{2}\,(\nabla\phi^{(2)})^2\,d\Omega + \iint_{S_f+S_B+S_R} f(\phi^{(2)})\,dS \qquad (23)$$

where:

$\Omega$ = fluid domain

$S_f$ = free surface

$S_B$ = body boundary

$S_R$ = boundary for the radiation condition

The integral ($\iint_{s_f}$) over the unknown free surface in Equation 23 may be approximated by a Taylor series expansion, in terms of the variables at the mean sea surface.

Solutions for the second-order diffraction and radiation boundary value problems may be formulated using the standard finite element method. The radiation boundary condition is imposed on a finite boundary, $\Gamma_2$, at moderate distances from the structures of interest. The entire fluid inside this boundary is divided into two regions. Each region has the functionals corresponding to its respective governing equations and associated boundary conditions as follows:

For the three-dimensional region:

$$\Pi^{(2)} = \iiint_{\Omega_1} \frac{1}{2} (\nabla \phi_j^{(2)})^2 \, d\Omega - \iint_{S_f} 2 \frac{\omega^2}{g} (\phi_j^{(2)})^2 \, dS$$

$$- \iint_{S_f} \frac{Q(x,y,0)}{g} \phi_j^{(2)} \, dS - \iint_{S_s} (v_n)_{im}^{(2)} \cdot \delta_{km} \phi_{ik}^{(2)} \, dS_k \tag{24}$$

$$+ \iint_{S_s} [(\vec{x}^{(1)} \cdot \nabla) \nabla \phi^{(1)} \vec{n} + (\vec{v}^{(1)} - \nabla \phi^{(1)}) \cdot \vec{N}^{(1)}]_{im} \cdot \delta_{km} \phi_{ik}^{(2)} \, dS_k$$

$j$ = II,D+S,i,k,...
$i$ = 1,2,...6
$k$ = 1,2,...M

where M is the total number of floating bodies and $\phi_{ik}^{(2)}$ is that of the radiated waves due to motion in the $i^{th}$ mode by the $k^{th}$ body, in which $i=1,2,\ldots,6$ corresponds to the surge, sway, heave, roll, pitch, and sway modes, respectively. The quantity Q in the third term in the above equation is given in Equation 15.

For the two-dimensional region:

$$\Pi^{(2)} = \iint_{\Omega_2} \frac{1}{2} \left\{ F^* (\nabla \phi_j^{(2)})^2 - 4 k^2 F^* (\phi_j^{(2)})^2 \right\} d\Omega_2$$

$$- \int_{\Gamma_1} F^* \frac{\partial \phi_{II}^{(2)}}{\partial n} \phi_j^{(2)} \, dS + (\text{Radiation Condition for } \phi_S^{(2)}), \quad j = II,D+S,i,k... \tag{25}$$

The function F* in Equation 25 is the function defined by Equation A-22 of Appendix A.

On $\Gamma_1$, the three-dimensional region is coupled with the two-dimensional region by the following relationship:

$$\phi_j^{(2)}(x,y,z) = \phi_j^{(2)}(x,y) \frac{\cosh 2k(d+z)}{\sinh^4 (kd)}, \qquad j = II,S+D,i,k \tag{26}$$

where d is the water depth.

## FINITE ELEMENT DISCRETIZATION

The integral Equations 24 and 25 define the velocity potentials of the water flow over the entire fluid domain. The fluid and boundaries are thus discretized, as shown in Figure 2, to conform the finite element applications.

The potential $\phi^{(2)'}$ within each element can be approximated in terms of the unknown nodal values $\{\phi_e^{(2)}\}$ of that element and interpolation functions [N]. In matrix notation:

$$\phi^{(2)'} = [N]\left\{\phi_e^{(2)}\right\} \tag{27}$$

The functional $\Pi^{(2)}$ is now minimized with respect to the nodal values $\phi_e^{(2)}$ for a single element to determine the flow potential which satisfies the boundary value problem. For the 3-dimensional case, Equation 27 can be inserted into Equation 24 and written as:

$$\delta\,\Pi^{(2)} = \frac{\partial \Pi^{(2)}}{\partial \phi_e^{(2)}}\,\delta\,\phi_e^{(2)} = 0 \tag{28}$$

This being true for any variation, $\delta\,\phi_e^{(2)}$ requires:

$$\frac{\partial \Pi^{(2)}}{\partial \phi_e^{(2)}} = \begin{Bmatrix} \partial \Pi^{(2)}/\partial(\phi_e^{(2)})_1 \\ \partial \Pi^{(2)}/\partial(\phi_e^{(2)})_2 \\ \vdots \\ \partial \Pi^{(2)}/\partial(\phi_e^{(2)})_n \end{Bmatrix} = 0 \tag{29}$$

from which parameters $\{\phi_e^{(2)}\}$ are to be determined. Because the functional is quadratic, element Equation 29 reduces to a standard linear algebraic equation, that is:

$$\frac{\partial \Pi^{(2)}}{\partial \phi_e^{(2)}} = [k]\left\{\phi_e^{(2)}\right\} - \{f\} = 0 \tag{30}$$

This transforms the integral equations into a set of linear algebraic equations in the unknown value of velocity potential at boundary nodes on all elements.

### Stiffness Matrix and Nodal Force Vector for the 3D Element

The element stiffness matrix [k] and the element nodal force vector {f} in Equation 30 are given as:

$$[k] \;=\; \iiint_{(\Omega)_e} (\nabla N)^T (\nabla N)\, dx\, dy\, dz \;-\; \iint_{(S_f)_e} \frac{4\,\omega^2}{g}\, N^T N\, dS \tag{31}$$

$$\begin{aligned} \{f\} \;=\; & -\iint_{(S_k)_e} N^T (v_n)_{ik}\, dS \cdot \delta_{km} \\ & + \iint_{S_e} N^T \Big[ (x^{(1)} \nabla)\, \nabla \phi_j^{(1)} \cdot n \;+\; (v^{(1)} - \nabla \phi_j^{(1)}) \cdot N^{(1)} \Big] dS \cdot \delta_{km} \\ & + \iint_{S_f} N^T \frac{Q}{g}\, dS \end{aligned} \tag{32}$$

$v_n$ = normal velocity

$x^1$ = the first order displacements

In the above equation, $\Omega_e$ and $S_e$ denote that corresponding integrations are taken over a single element only. The velocity potential, $\phi_e^{(2)}$, at boundary nodes of a single element consists of three components. These are incident, scattered, and radiated potentials. Hence, the element equations can be written as:

$$[k]\left\{\phi_e^{(2)}\right\} \;=\; \{f\}_j\,; \qquad j = \Pi, S{+}D, i, k \tag{33}$$

### Stiffness Matrix and Nodal Force Vector for the 2D Element

Similarly, the element equation for the 2D case can be derived by taking the differentiation on the functional $\Pi^{(2)}$ given in Equation 25 with respect to $\phi_e^{(2)}$. Then:

$$\frac{\partial \Pi^{(2)}}{\partial \phi_e^{(2)}} = \int\int_{(\Omega_2)_e} \{(\nabla N)^T F^* (\nabla N) - 4\,k^2 F^* N^T N\}\, dx\, dy \cdot \phi_e^{(2)}$$

$$- \int_{(\Gamma_2)_e} F^* \frac{\partial \phi_{II}^{(2)}}{\partial n} N^T dS \qquad (34)$$

$$+ \int_{(\Gamma_2)_e} F^* \left\{ \alpha\, N^T N + \beta \left(\frac{\partial N}{\partial S}\right)^T \left(\frac{\partial N}{\partial S}\right) \right\} dS \cdot \phi_e^{(2)} = 0$$

and a system of equations for the problem is:

$$[k(x,y)] \left\{\phi_e^{(2)}\right\}_j = \{f(x,y)\}_j\,; \qquad j = \mathrm{II}, S+D, i, k \qquad (35)$$

with

$$[k(x,y)] = \int\int \{(\nabla N)^T F^* (\nabla N) - 4\,k^2 F^* N^T N\}\, dx\, dy$$
$$+ \int F^* \left\{ \alpha\, N^T N + \beta \left(\frac{\partial N}{\partial S}\right)^T \left(\frac{\partial N}{\partial S}\right) \right\} dS \qquad (36)$$

$$\{f(x,y)\} = \int F^* \frac{\partial \phi_{II}^{(2)}}{\partial n} N^T dS \qquad (37)$$

Equations deducted from the 2D and 3D elements can be assembled to form a set of global equations pertaining to the entire fluid region. These may be written in matrix form as:

$$[K]\{\phi^{(2)}\} = \{F\} \qquad (38)$$

The global stiffness matrix [K] is symmetric and banded. Its half-bandwidth indicates interactions between nodes of an element and its immediate neighbors. Equation 38 may now be solved numerically.

## SECOND-ORDER WAVE LOADS ON A FLOATING BODY

Once the second-order velocity potential is determined, the second-order wave loading on the floating body can be calculated. It is assumed that the vessel undergoes small first-order motions $\vec{X}^{(1)}$ from its mean position $\vec{X}^{(0)}$, and that the pressure can be expanded in a Taylor series about the hydrostatic pressure at the mean position and the following expression is found:

$$p = p^{(0)} + \varepsilon p^{(1)} + \varepsilon^2 p^{(2)} + O(\varepsilon^3) \tag{39}$$

where:

hydrostatic pressure: $p^{(0)} = -\rho g Z^{(0)}$ (40)

first-order pressure: $p^{(1)} = -\rho g Z^{(1)} - \rho \Phi_t^{(1)}$ (41)

second-order pressure: $p^{(2)} = -\dfrac{1}{2}\rho |\vec{\nabla}\Phi^{(1)}|^2 - \rho \Phi_t^{(2)} - \rho\left(\vec{X}^{(1)} \cdot \vec{\nabla}\Phi_t^{(1)}\right)$ (42)

The total hydrodynamic force exerted on the body relative to the coordinate system $G\hat{x}\hat{y}\hat{z}$ is given by the following equation:

$$\vec{F} = -\iint_S p \vec{N} dS \tag{43}$$

where S is the instantaneous wetted surface and $\vec{N}$ is the instantaneous normal vector to the surface element dS relative to system $G\hat{x}\hat{y}\hat{z}$.

$$\vec{N} = \vec{N}^{(0)} + \varepsilon N^{(1)}$$

Substitution of the pressure p given by Equation 39 and retaining the integration to the second order, one obtains:

$$\vec{F} = \vec{F}^{(0)} + \varepsilon \vec{F}^{(1)} + \varepsilon^2 \vec{F}^{(2)} + O(\varepsilon^3) \tag{44}$$

The instantaneous wetted surface S is composed of two parts, $S_0$ and s (Figure 2). $S_0$ is the constant wetted surface up to the still water line and s is the surface between the still water line and the wave profile along the vessel.

The second-order forces can be calculated by integrating all products of pressure p and normal vector $\vec{N}$ which give second-order force contributions over the wetted surface $S_0$ and s:

$$\vec{F}^{(2)} = -\iint_{S_0} \left( p^{(1)} \vec{N}^{(1)} + p^{(2)} \vec{n} \right) dS - \iint_{s} p^{(1)} \vec{n} \, dS \tag{45}$$

Substituting

$$\vec{N}^{(1)} = \vec{\theta}^{(1)} \times \vec{n}$$

into the above equation yields for the first term

$$-\iint_{S_0} p^{(1)} \vec{N}^{(1)} dS = \vec{\theta} \times -\iint_{S_0} p^{(1)} \vec{n} \, dS = \vec{\theta} \times \vec{F}^{(1)} \tag{46}$$

where $\vec{F}^{(1)}$ is first-order wave exciting force and hydrodynamic reaction force. According to Newton's second law, $\vec{F}^{(1)}$ can be written as:

$$\vec{F}^{(1)} = [M] \ddot{\vec{X}}_G^{(1)} \tag{47}$$

where [M] is mass of vessel in the air and $\vec{X}_G^{(1)}$ is the first-order acceleration of the center of gravity of the body. Thus, the first term of the second-order force may be obtained from the first-order motion dynamics as:

$$-\iint_{S_0} p^{(1)} \vec{N}^{(1)} dS = \vec{\theta}^{(1)} \times [M] \vec{X}_G^{(1)} \tag{48}$$

The second term of the second-order forces is integrated numerically. The following was obtained from Equation 45:

$$-\iint_{S_0} p^{(2)} \vec{n} \, dS = \rho \iint_{S_0} \left[ \frac{1}{2} |\vec{\nabla} \Phi^{(1)}|^2 + \Phi_t^{(2)} + \vec{X}^{(1)} \cdot \vec{\nabla} \Phi_t^{(1)} \right] \vec{n} \, dS \tag{49}$$

The integral of the oscillating surface s is calculated to the linearized free surface by substituting $p^{(1)}$ from Equation 41:

$$-\iint_{s} p^{(1)} \vec{n} \, dS = -\iint_{s} \left(-\rho g Z^{(1)} - \rho \Phi_t^{(1)}\right) \vec{n} \, dS \tag{50}$$

where the surface element is written as:

$$dS = d Z^{(1)} \cdot dl \tag{51}$$

At the still water line, the linearized free surface condition to first order is:

$$-\rho \Phi_t^{(1)} = \rho g \zeta^{(1)} \tag{52}$$

where $\zeta^{(1)}$ is the first-order free surface elevation. Inserting Equations 51 and 52 into Equation 50 results in the following:

$$-\iint_{s} p^{(1)} \vec{n} \, dS = -\int_{WL} \frac{1}{2} \rho g \left(\zeta_r^{(1)}\right)^2 \vec{n} \, dl \tag{53}$$

in which $\zeta_r^{(1)}$ is the relative wave elevation defined by:

$$\zeta_r^{(1)} = \zeta^{(1)} - Z_{WL}^{(1)} \tag{54}$$

The final expression for the total second-order force thus becomes:

$$\begin{aligned} \vec{F}^{(2)} = & -\int_{WL} \frac{1}{2} \rho g \left(\zeta_r^{(1)}\right)^2 \vec{n}_G \, dl + \vec{\theta}^{(1)} \times [M] \vec{X}_G^{(1)} \\ & -\iint_{S_0} \left[-\frac{1}{2} \rho \, |\vec{\nabla} \Phi^{(1)}|^2 - \rho \Phi_t^{(2)} - \rho\left(\vec{X}^{(1)} \cdot \vec{\nabla}\Phi_t^{(1)}\right)\right] \vec{n} \, dS \end{aligned} \tag{55}$$

The second-order force given in Equation 49 can be divided into a steady component and a time-dependent biharmonic wave exciting force. The steady component is a second-order steady wave drift force calculated from Equation 49 by taking the time average over one wave period. Since the flow is periodic, the time average value of $\zeta_r$ is zero. As a result, the second-order steady wave drift force becomes:

$$\begin{aligned} f_D^{(2)} = \overline{\vec{F}^{(2)}} = & - \int_{WL} \overline{\frac{1}{2} \rho g \left(\zeta_r^{(1)}\right)^2 \vec{n}\, dl} + \overline{\vec{\theta}^{(1)} \times [M] \vec{X}_G^{(1)}} \\ & + \rho \iint_{S_0} \overline{\left[ \frac{1}{2} |\nabla \Phi^{(1)}|^2 + \Phi_t^{(2)} + \left( X^{(1)} \cdot \nabla \Phi_t^{(1)} \right) \right] \vec{n}\, dS} \end{aligned} \tag{56}$$

For regular waves

$$\rho \iint_{S_0} \overline{\Phi_t^{(2)} \vec{n}\, dS} = 0$$

Thus, the second-order force can be written as:

$$\vec{F}^{(2)} = \vec{f}_D + R_e \left\{ f^{(2)} e^{i 2 \omega t} \right\} \tag{57}$$

where $f^{(2)}$ is the second-order biharmonic wave force and is given by:

$$\begin{aligned} \vec{f}^{(2)} = & - \int_{w} \frac{\rho\, \omega^2}{4 g} (\phi_r^{(1)})^2 \vec{n}\, dl + \vec{\theta}^{(1)} \times [M]\, \vec{\chi}_G^{(1)} \\ & \iint \left[ \frac{1}{4} \rho (\nabla \phi^{(1)})^2 + 2 i \omega \rho \phi^{(2)} + 2 i \omega \rho (\vec{\chi}^{(1)} \cdot \nabla \phi^{(1)}) \right] \vec{n}\, dS \end{aligned} \tag{58}$$

where:

$$\Phi^{(1)} = \phi^{(1)} e^{i\omega t}$$

$$\Phi^{(2)} = \phi^{(2)} e^{i\omega t}$$

$$\vec{X}_G^{(1)} = \vec{\chi}_G^{(1)} e^{i\omega t}$$

$$\vec{\Theta}^{(1)} = \vec{\theta}^{(1)} e^{i\omega t}$$

$$\zeta_\gamma^{(1)} = \phi_\gamma^{(1)} e^{i\omega t}$$

The total hydrodynamic moment about the center of gravity of the vessel relative to the coordinate system $G\hat{x}\hat{y}\hat{z}$ is given by Equation 5:

$$\vec{M} = -\iint_S p(\vec{X} \times \vec{N})\, dS \tag{59}$$

The derivation is analogous to that followed for the forces. The final expression for the second-order wave moment is:

$$\begin{aligned} \vec{M}^{(2)} = & -\int_{WL} \frac{1}{2} \rho\, g \left(\zeta_r^{(1)}\right)^2 (\vec{x} \times \vec{n})\, dl + \vec{\theta}^{(1)} \times [I]\, \vec{\theta}^{(1)} \\ & -\iint_{S_0} \left[ -\frac{1}{2} \rho\, |\vec{\nabla} \Phi^{(1)}|^2 - \rho\, \Phi_t^{(2)} - \rho\left(\vec{X}^{(1)} \cdot \vec{\nabla} \Phi_t^{(1)}\right) \right] (\vec{x} \times \vec{n})\, dS \end{aligned} \tag{60}$$

## EXPERIMENTAL STUDY

### Test Setup and Procedures

A hydraulic model was designed to observe the coupling process of a fixed barge with nonlinear waves in shallow water. The experiment was conducted in a two-dimensional wave tank at the Civil Engineering Laboratory of Texas A&M University. Figure 4 illustrates the general setup of the experiment. The tank was 36 meters long, 0.91 meter wide, and 1.22 meters deep. The water depth was maintained at a constant of 20.3 cm throughout the entire experiment. A rectangular box (101.6 cm by 33.9 cm by 8.4 cm) was placed at roughly 11 meters from the wavemaker and centered in the tank, to simulate a barge afloat at the water

surface. The box was mounted to a rigid aluminum frame with three legs as shown in Figure 4. The box was further ballasted to a neutrally buoyant condition at the draft of 8.4 cm in the still water

Two load cells were placed at the end of each of the three legs to measure the horizontal and vertical forces, respectively. Each cell provided a capacity of 50 pounds at an accuracy of ±1 percent of the force applied. The total forces and moments were deduced from these measurements.

A significant influence on the wave activity around the test model due to the close proximity of side walls of a narrow wave tank is anticipated. The wave forces imposed on the test model will be different from those experienced in an otherwise open water. However, this test was intended for validating the numerical procedure. The side walls of the wave tank were simulated in the numerical procedure to give a fair comparison between the physical and numerical models.

The experimental waves were generated by a computer-controlled Commercial Hydraulics RSW 90-85 dryback, hinged-flap wavemaker. The water pumped by the flap traveled down the tank channel and evolved into shallow water Cnoidal waves before it reached the barge. Two resistance-type wave gauges were used to monitor the wave profiles. One was placed at 75 cm forward of the bow along the center line of the tank, and the other at 47 cm aft of the bow, centered between the box and the side of the tank. The accuracy of the gauges was ±1 mm. Four wave periods were selected intentionally to avoid the resonance frequency of the wave tank. Six wave heights in the range that promised results of well defined Cnoidal wave profiles were chosen for each wave period. The wave parameters used in the test are summarized in Table 1. The Ursell number of these waves varied from 0.5 to 70.

Data acquisition was accomplished using a Hewlett Packard HP-3852A data acquisition/control unit with an HP-330 workstation. This system was equipped with a 10-channel relay multiplexer (HP-44718A) and an integrating voltmeter operating at a 5-1/2-digit resolution (HP-44701A). Details of the test setup and procedures are described in Reference 14.

**Test Results**

Twenty-four sets of time history of the wave profiles and the horizontal and vertical forces were recorded. A sample set of these measurements is shown in Figure 5. The incident wave elevation shows good agreement with that predicted by the Cnoidal wave theory in both wave height and period. However, it is noted that the experimental wave is asymmetric in contrast to the asymmetric mathematical form. This discrepancy grows as the wave height increases. This results from the wave generation mechanism used in the test. The force time histories are similar in shape to that of the wave profile. The time histories of all measurements are decomposed by Fast Fourier transform up to the third harmonic as follows:

$$X(t) = X_o + \sum_{n=1}^{3} \frac{X_n}{2} \cos(n\omega t + e_n)$$

where:

$X_0$ = the mean value

$X_n$ = height of the nth harmonic component

$e_n$ = the phase angle

$\omega$ = base frequency

The symbols H, X, and Z represent the wave height and the double amplitudes of the forces in the horizontal and vertical directions, respectively.

It was found that all the mean values and the third harmonics were negligibly small in comparison to the first and the second harmonics, and are therefore not discussed. The results of decomposition of the waves are shown in Figure 6. The height ratios of each harmonic component to the resultant wave height were plotted versus the resultant wave height. The same ratios deduced from the theoretical Cnoidal waves are presented in dashed lines in the same plots for comparison with the measurements. The measurements are almost identical with their theoretical counterparts. It is noted that, for the short period waves, the height ratios remain essentially constant over the range of the total wave height considered. For the long period waves, these ratios vary nonlinearly with the increase of total wave height with the first harmonic component decreases and the second harmonic increases. This result clearly demonstrates the typical nonlinear characteristics of the shallow water waves.

The force time histories are decomposed likewise. For convenience, the components are further nondimensionalized in the form of force coefficients as follows:

$$C_x = \frac{X_1}{\rho H_1 lb}$$

$$C_z = \frac{Z_1}{\rho H_1 lb}$$

where $\rho$ is the specific weight of water and "l" and "b" are the length and the beam of the box, respectively. These force coefficients are equivalent to the ratios of the heights of the first harmonic forces to the first harmonic wave height. Figure 7 indicates that these coefficients remain constant at a specific wave period. This implies that the heights of the first harmonic forces are linearly correlated to the height of the first harmonic wave. The second harmonic terms $H_2$, $X_2$, $Z_2$ are plotted as functions of the first harmonic wave height $H_1$ squared as shown in Figure 8. The units are given in cm for $H_2$, Newtons for force harmonics, and $cm^2$ for $H_1^2$. The results, which closely fit the first-order regression line, indicate that the second harmonic terms $X_2$, $Z_2$, and $H_2$ are linearly correlated to the square of the first harmonic wave height.

The proportionality constants for $X_2$ monotonically increase as the wave period increases, whereas the constants for $Z_2$ generally increase but slightly fluctuate. The proportionality

constants for $H_2$ increase as the wave period increases, although the constants are generally very small compared to those of the forces.

**Nondimensional Forces and Wave Heights Versus the Ursell Number**

The first and second harmonics of the forces and incident wave height are nondimensionalized by dividing them by their respective resultants, then compared to the Ursell number,

$$U_r = \frac{HL^2}{h^3}$$

where h = water depth. The first harmonic ratios exhibit a linear trend and the second harmonic ratios present some nonlinearity, as shown in Figure 9. $H_1/H$ and $X_1/X$ decrease linearly as the Ursell number increases while $Z_1/Z$ remains constant. $H_2/H$ and $X_2/X$ increase initially then approach to a constant value while $Z_2/Z$ decreases slightly throughout the range of Ursell numbers. This trend seems to agree with the previous finding shown in Figure 10 from Sarpkaya and Isaacsson (Ref 15) on nonlinear shallow water wave forces on a vertical circular cylinder.

## NUMERICAL RESULTS

The finite element procedure derived in the previous section on theoretical considerations was executed in a computer program, NAUTILUS, coded in standard Fortran 77 language. This procedure discretized the water body under consideration with a combination of three- and two-dimensional finite element meshes. This feature permitted optimization of computer resources while retaining the essential details of the physical problem under study. The discretization resulted in a linear matrix, Equation 38, which was treated by a proven procedure based on the frontal method developed by Irons (Ref 16). The solution gave a complete description of the fluid activity in terms of velocity potentials. NAUTILUS presents the results in a convenient form for practical application, including wave height distribution over the entire water surface, wave-induced forces on the fixed structures, and the dynamic motion of the floating structures. All computations are executed to the second harmonic.

NAUTILUS was used to reproduce the hydraulic model test described in the previous section on experimental study. The results were used to verify the feasibility of the NAUTILUS program. Since NAUTILUS does not include a wave generation mechanism to simulate the wavemaker, the wave tank will be approximated with a channel of infinite length with a steady second-order Stokes' wave approaching from one end of the channel. The water body within three times of the barge length from the center of the barge is simulated with three-dimensional element meshes, while the rest is approximated with two-dimensional element meshes. The water body under consideration extends to a distance of ten barge lengths on each side. Figure 11 illustrates the discretization of the model test setup. Wave parameters used in the model test are entered into the numerical model for comparison with the forces observed from the model test.

The results of the wave forces predicted by the numerical model (in black symbols) are presented along with the hydraulic model measurements (in white symbols) in Figure 9. The fair agreement between the theoretical and the empirical results strongly supports the approach taken.

## CONCLUSIONS

A second-order simulation model for three-dimensional wave-structural couplings in moderate seas has been formulated. The results confirm the feasibility of reducing a weakly nonlinear free surface problem by the perturbation method. This treatment eliminates the need for specifying the unknown free surface, and allows the nonlinear problem to be addressed at the well-defined mean water surface in the perturbation components. Each component forms a well-defined linear boundary value problem that can be solved effectively. The present study solves the component boundary value problems with a finite element procedure. This procedure, which uses a combination of two- and three-dimensional finite elements, gives a good balance between computation efficiency and fair proximation of the physical problem.

The wave-induced forces on a rectangular box held steady at the water surface were studied both numerically and experimentally to examine the significance of the second-order forces. The second-order forces were found to increase with the Ursell number, $LH^2/h^3$, which is a measure of the wave steepness and the relative water depth, in a manner closely resembling the second-order profile of a Cnoidal eave. This implies that the significance of the second-order forces is similar to that of the second-order wave amplitude to the total amplitude of Cnoidal waves. Hydraulic model measurement indicates that the second-order lateral forces induced by steep waves in shallow water can be as large as 30 percent of the total lateral force. This confirms the importance of the second-order forces in high sea states. Actual wave forces experienced by ocean structures in rough seas can be much greater than those predicted by linear theories. More importantly, the additional wave forces may occur at frequencies away from the design wave frequency, and coincide with the resonance frequency of the structure of its components and cause adverse effects. Ocean structures for use in high sea states must be designed to withstand second-order forces.

## REFERENCES

1. M.Q. Issacson. "Nonlinear wave forces on large offshore structures," Journal of Waterways, Port, Coastal & Ocean Division, ASCE, vol 103, 1977, pp 166-170.

2. S.K. Chakrabarti. "Comments on second-order wave effects on a large diameter vertical cylinder," Journal of Ship Research, vol 22, 1978, pp 266-268.

3. B. Molin. "Second-order diffraction loads upon three-dimensional bodies," Applied Ocean Research, vol 1, 1979, pp 197-202.

4. J.V. Wehausen. "Perturbation methods in diffraction," Journal of Waterways, Port, Coastal & Ocean Division, ASCE, vol 106, 1980, pp 190-291.

5. J.N. Hunt and R.E. Baddour. "The diffraction of nonlinear progressive waves by a vertical cylinder," Quarterly Journal of Mechanical Applied Mathematics, vol 34, 1981, pp 69-87.

6. M.C. Chen and R.T. Hudspeth. "Nonlinear diffraction by eigenfunction expansions," Journal of Waterways, Port, Coastal & Ocean Division, ASCE, vol 108, 1982, pp 306-325.

7. M. Rahman. "Wave diffraction by large offshore structures; an exact second-order theory," Applied Ocean Research, vol 6, 1983, pp 90-100.

8. T.F. Ogilvie. "Second-order hydrodynamic effects on ocean platforms," International Workshop on Ship and Platform Motion, Berkeley, CA, 1983, pp 205-265.

9. M.H. Kim and D.K.P. Yue. "The complete second-order diffraction solution for an axisymmetric body," Part 1 - Monochromatic Incident Waves, Journal of Fluid Mechanics, vol 200, 1989, pp 235-264.

10. J.C.W. Berkhoff. "Linear wave propagation problems and the finite element method," Finite Elements in Fluids, vol 1, edited by R.H. Gallegher, et al., John Wiley & Sons, London, England, 1974, pp 251-280.

11. Naval Civil Engineering Laboratory. Memorandum to files on the interaction of ships with floating terminals, by T. Huang. Port Hueneme, CA, 1990.

12. J.V. Wehausen and E.V. Laitone. "Surface Wave," in Handbuch des Physik, Springer, Berlin, vol 9, 1960, pp 446-778.

13. F.B. Hildebrand. Method of applied mathematics, 2nd edition. Englewood Cliffs, NJ, Prentice-Hall, 1965.

14. G.S. Hook, C.H. Kim, and E.T. Huang. "Wave excitating forces on a platform fixed in nonlinear shallow water waves," in Proceedings of the International Conference, Civil Engineering in the Oceans V, College Station, TX, Nov 2-5, 1992, pp 311-325.

15. T. Sarpkaya and M. Isaacson. Mechanics of wave forces on offshore structures. New York, NY, Van Nostrand Publishing Co., 1981, pp 455-7.

16. B.B. Irons. "A frontal solution program for finite element analysis," International Journal of Numerical Mathematical Engineering, vol 2, 1970, pp 5-32.

Table 1
Wave Parameters Used for the Hydraulic Model Test

| $T_m$ (sec) | $H_m$ (cm) |
|---|---|
| 0.75 | 0.54, 1.09, 1.66, 2.11, 2.58, 3.13 |
| 1.00 | 0.52, 1.07, 1.60, 2.08, 2.55, 3.05 |
| 1.20 | 0.54, 1.52, 3.19, 5.09, 7.23, 9.23 |
| 1.58 | 0.69, 3.90, 4.98, 6.30, 8.48, 10.82 |

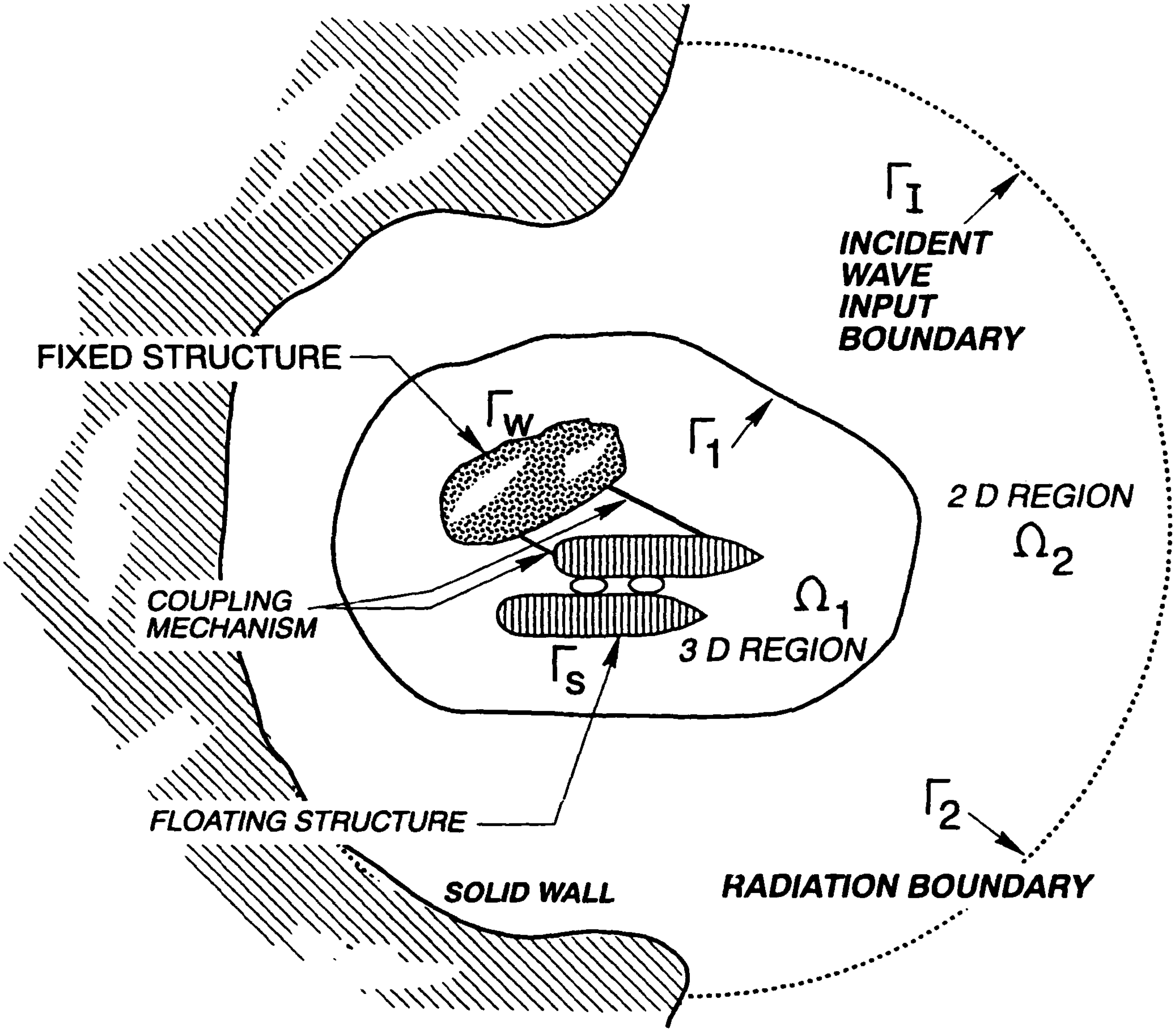


Figure 1
Definition sketch of a compound structure and the ambient fluid domains.

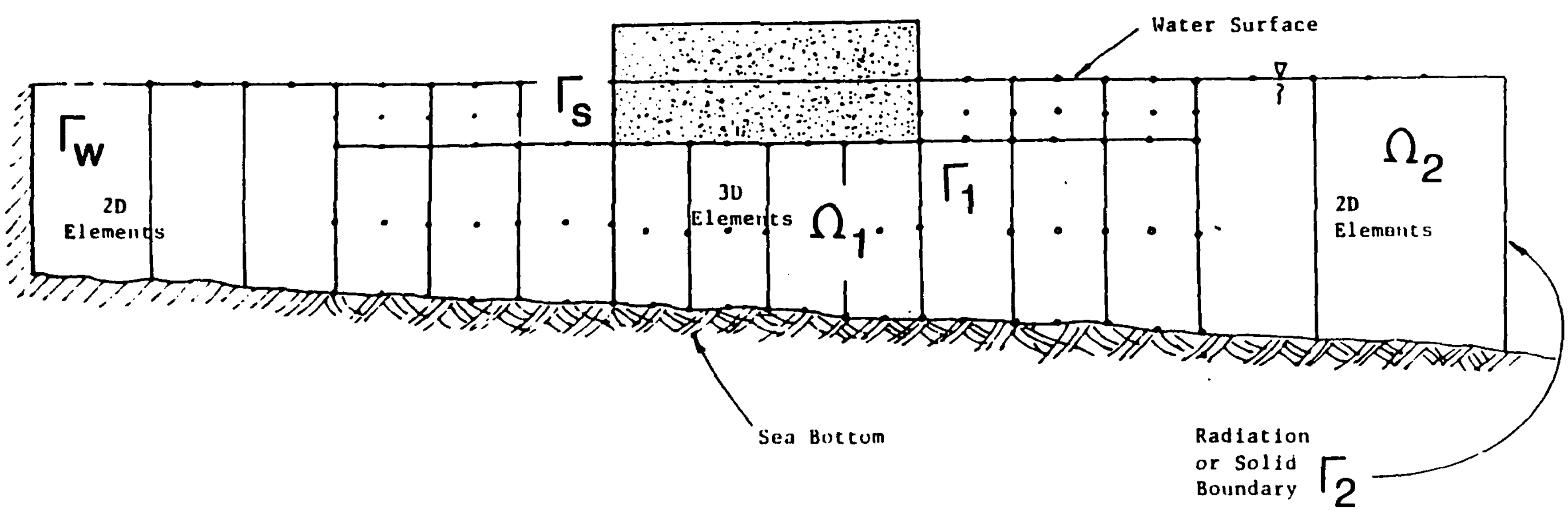


Figure 2
Coordinate systems.

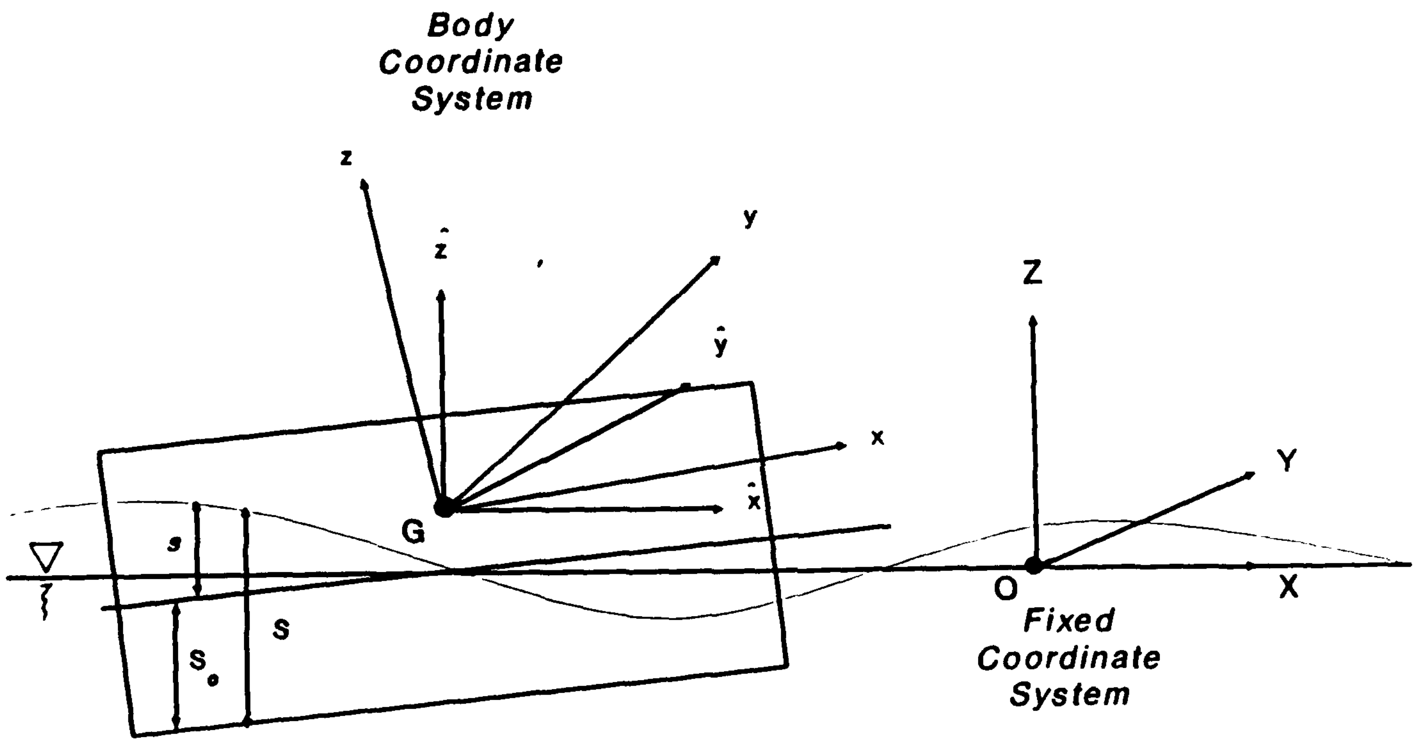


Figure 3
Finite element mesh.

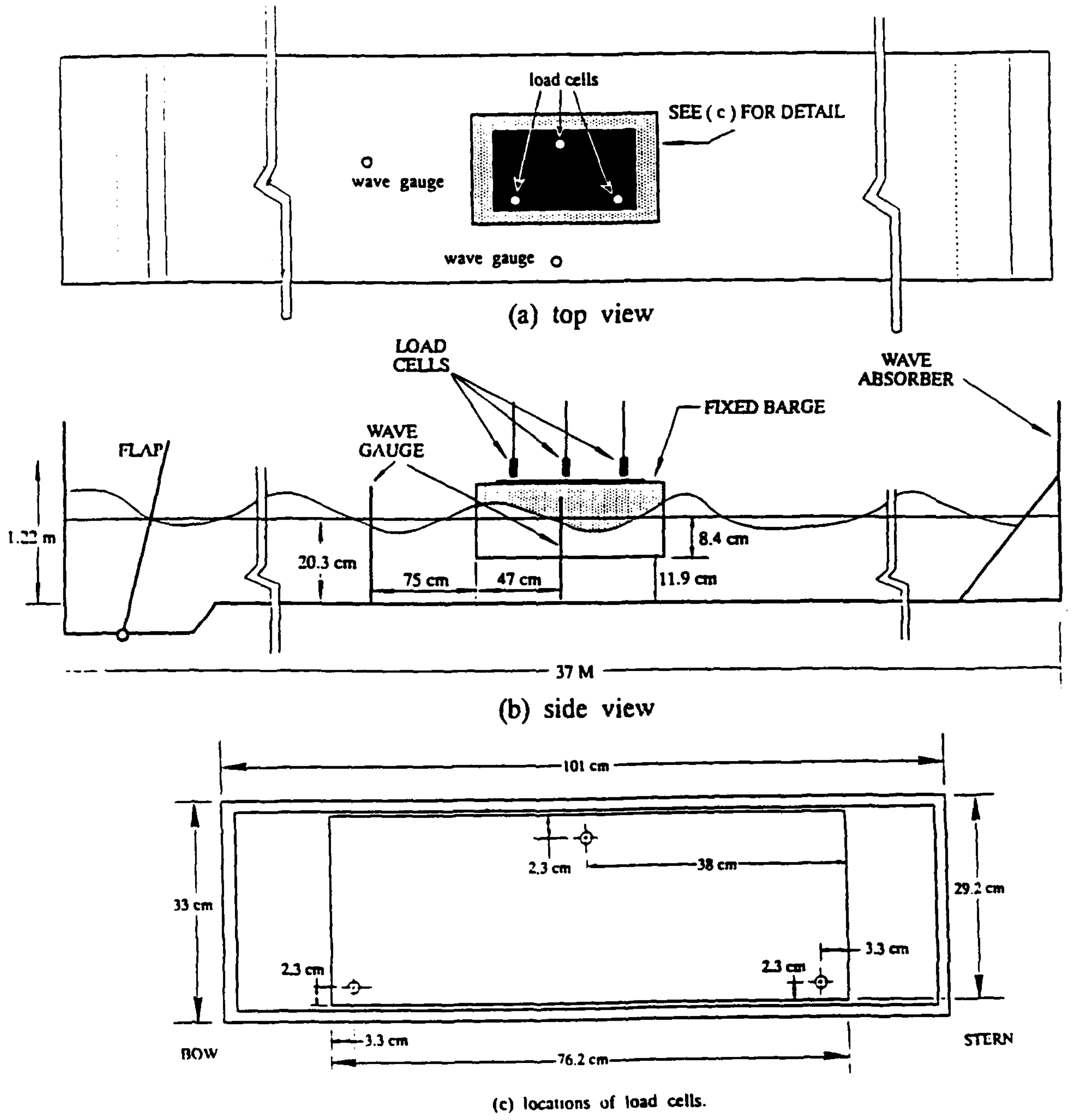


Figure 4
General layout of the hydraulic model.

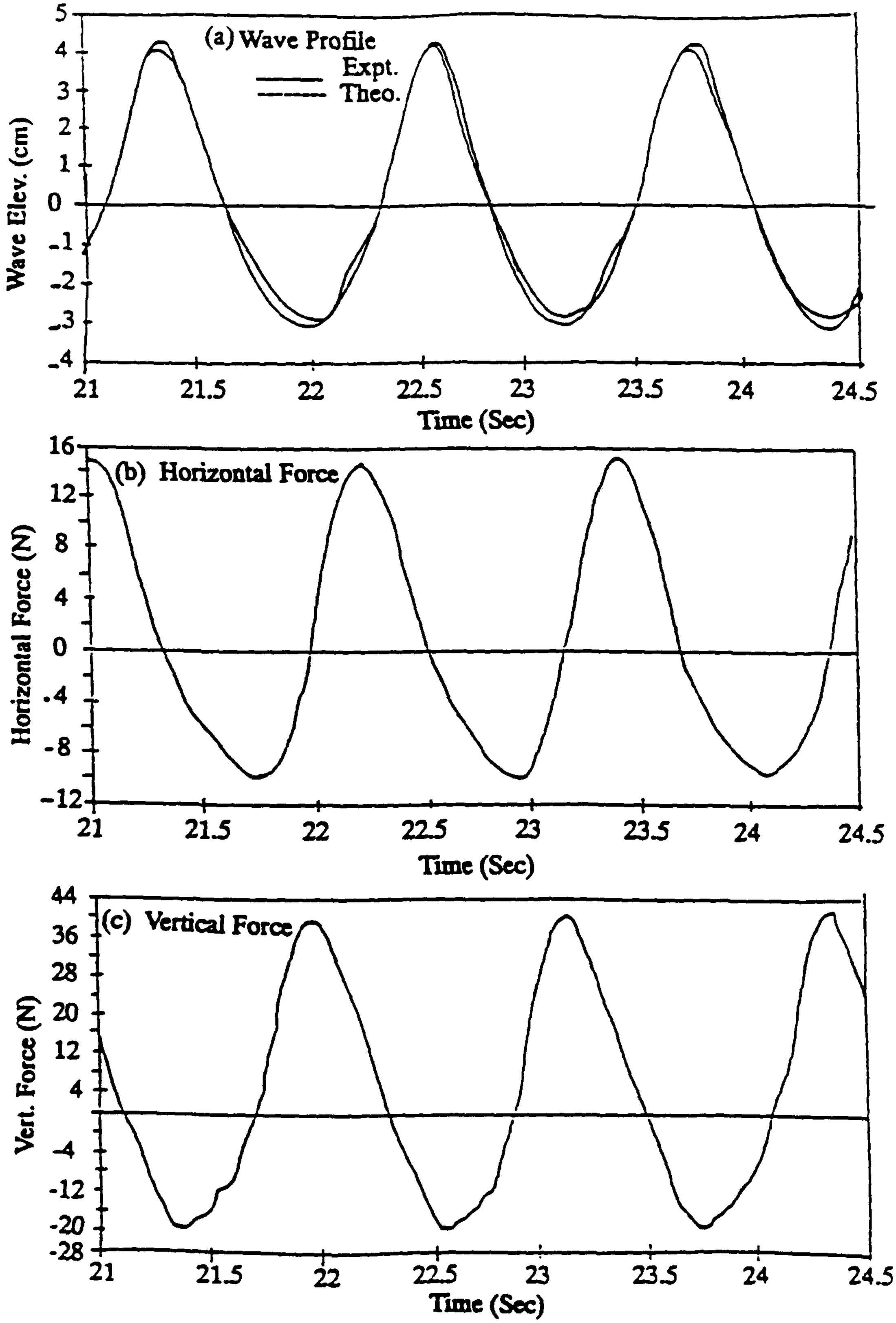


Figure 5
Profiles of sample incident wave height, horizontal force, and vertical force.

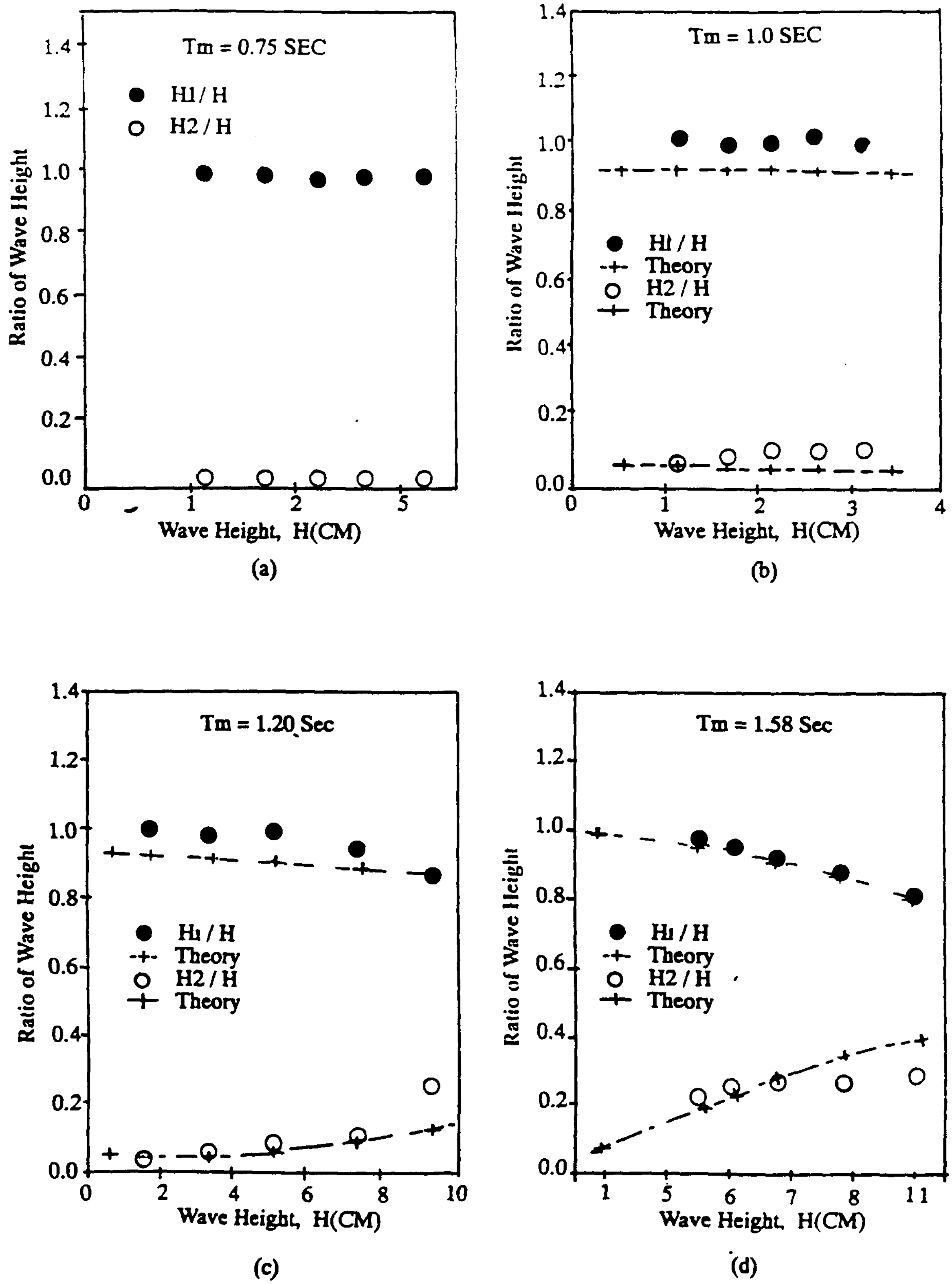


Figure 6
Decomposition of Cnoidal waves.

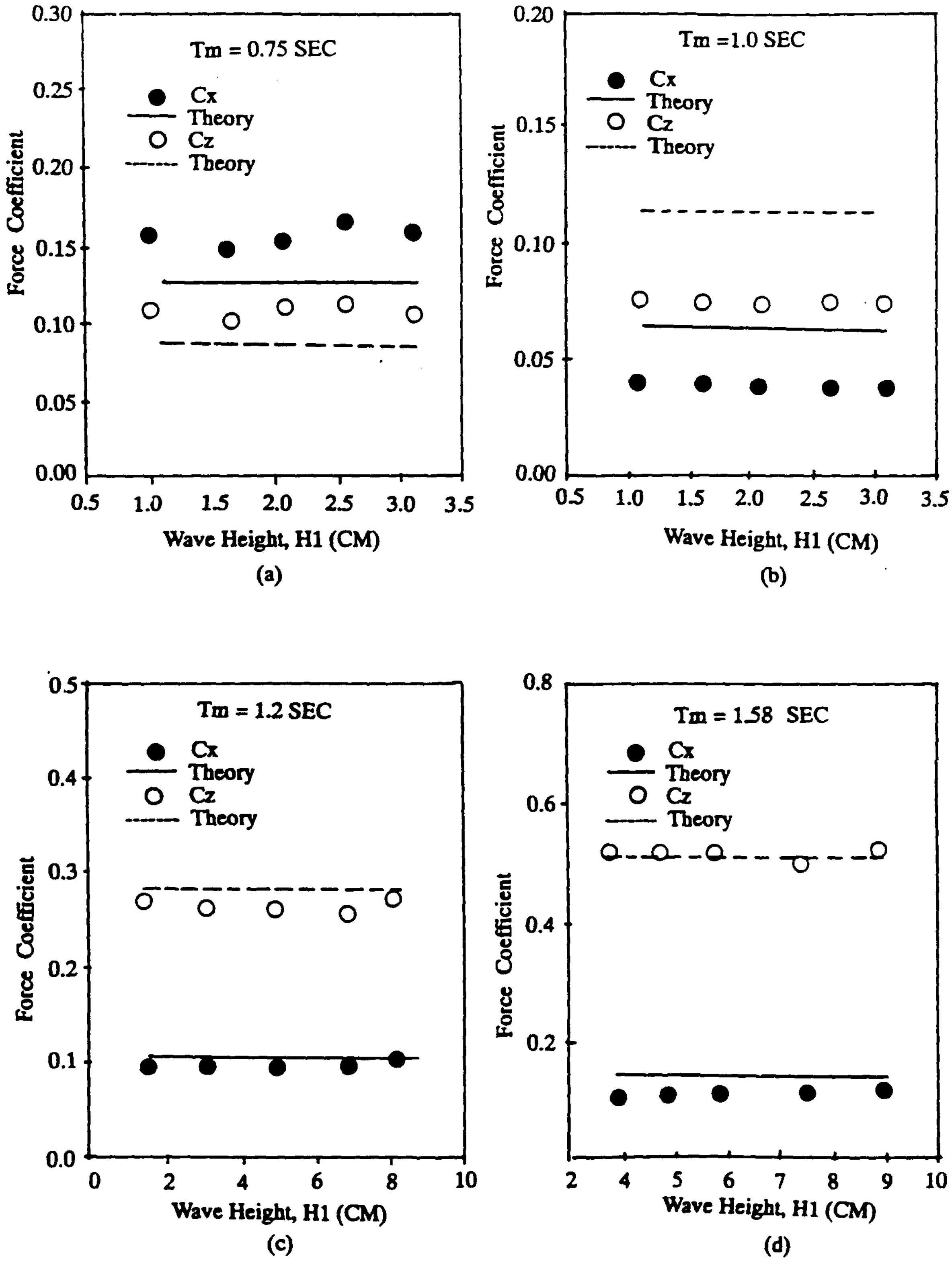


Figure 7
Hydraulic model measurements of the wave force coefficients.

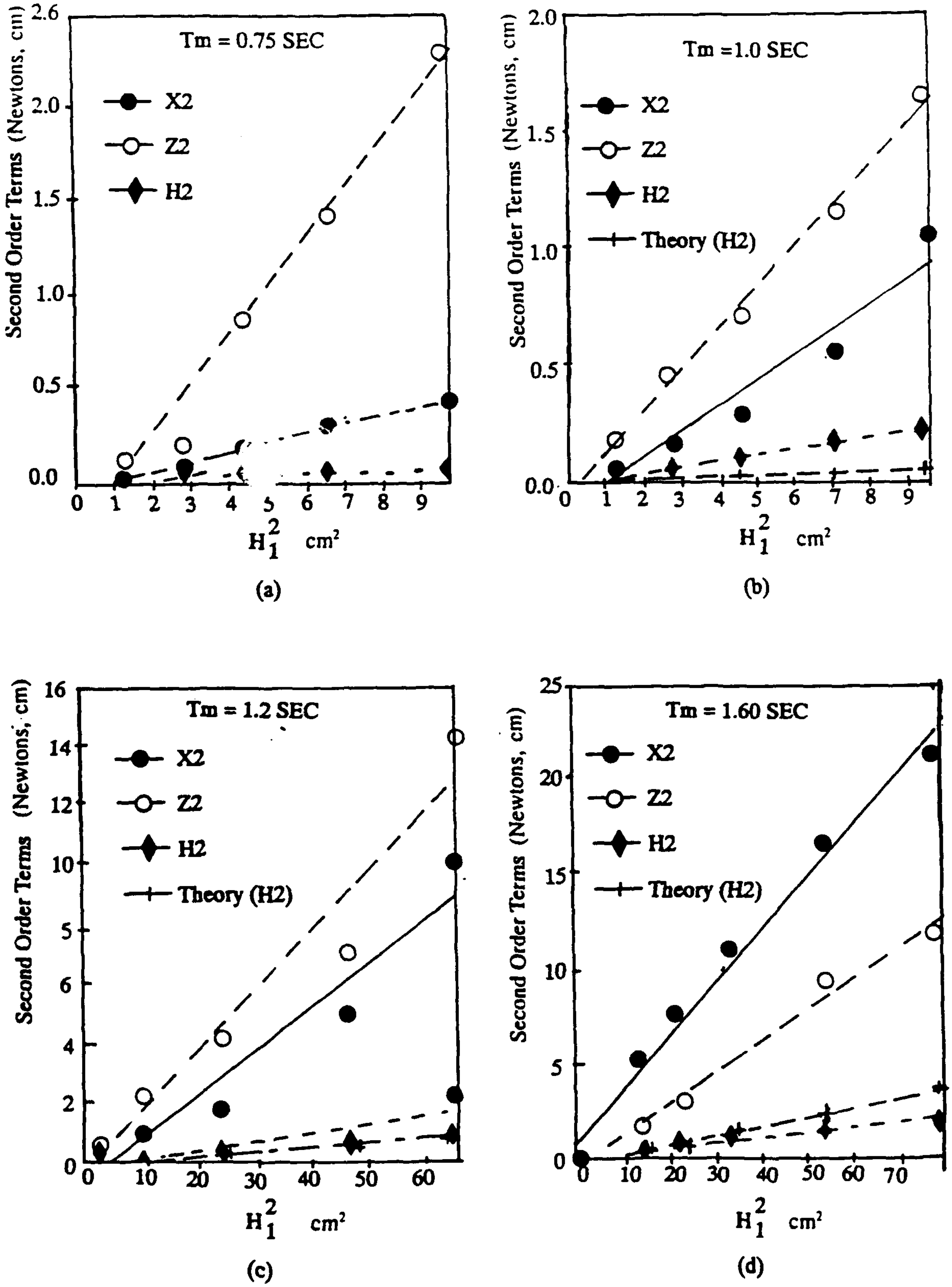


Figure 8
The second harmonics of the incident wave and wave forces.

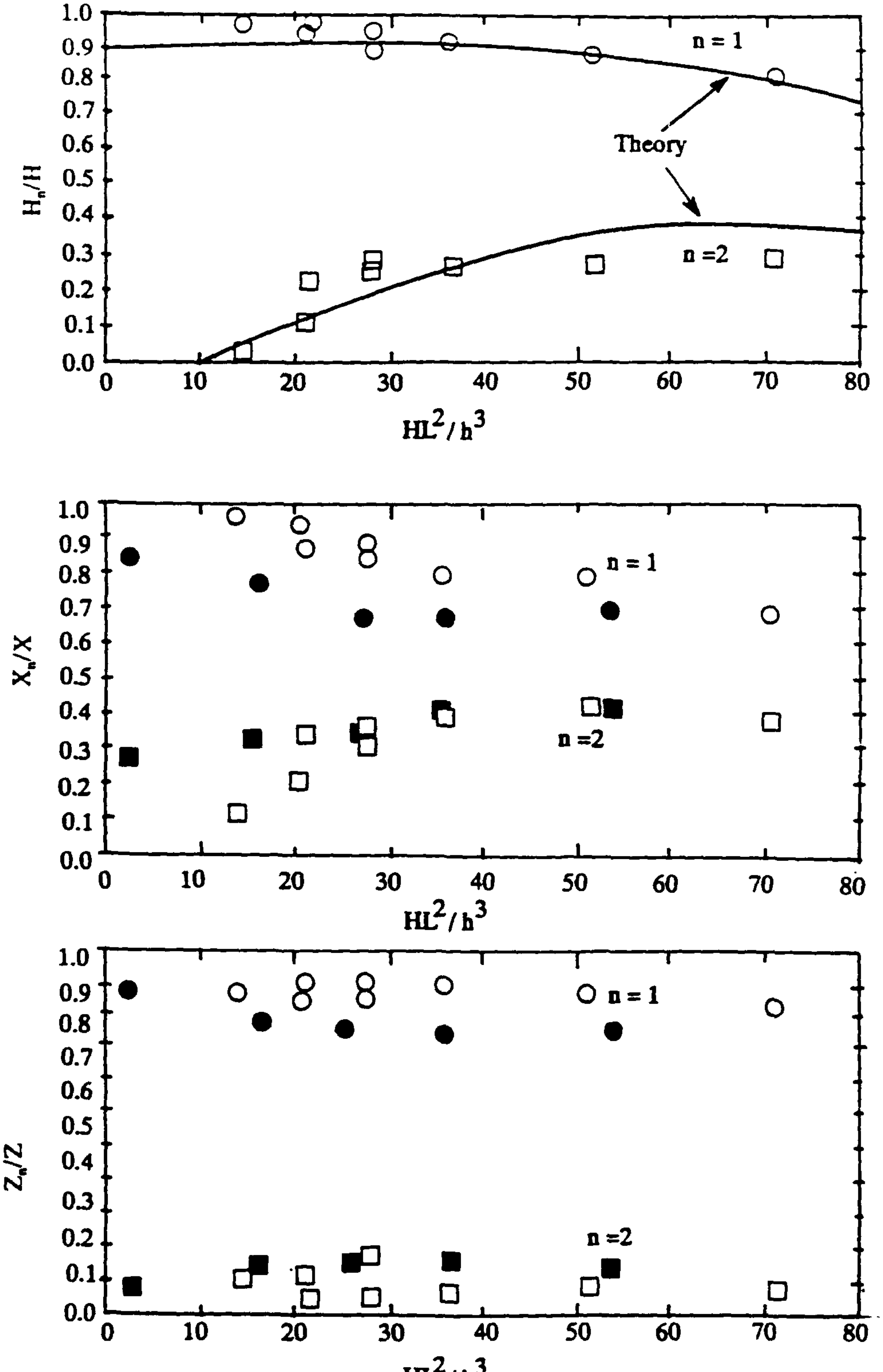


Figure 9
Fourier decomposition of incident waves and wave-induced force as a function of the Ursell number.

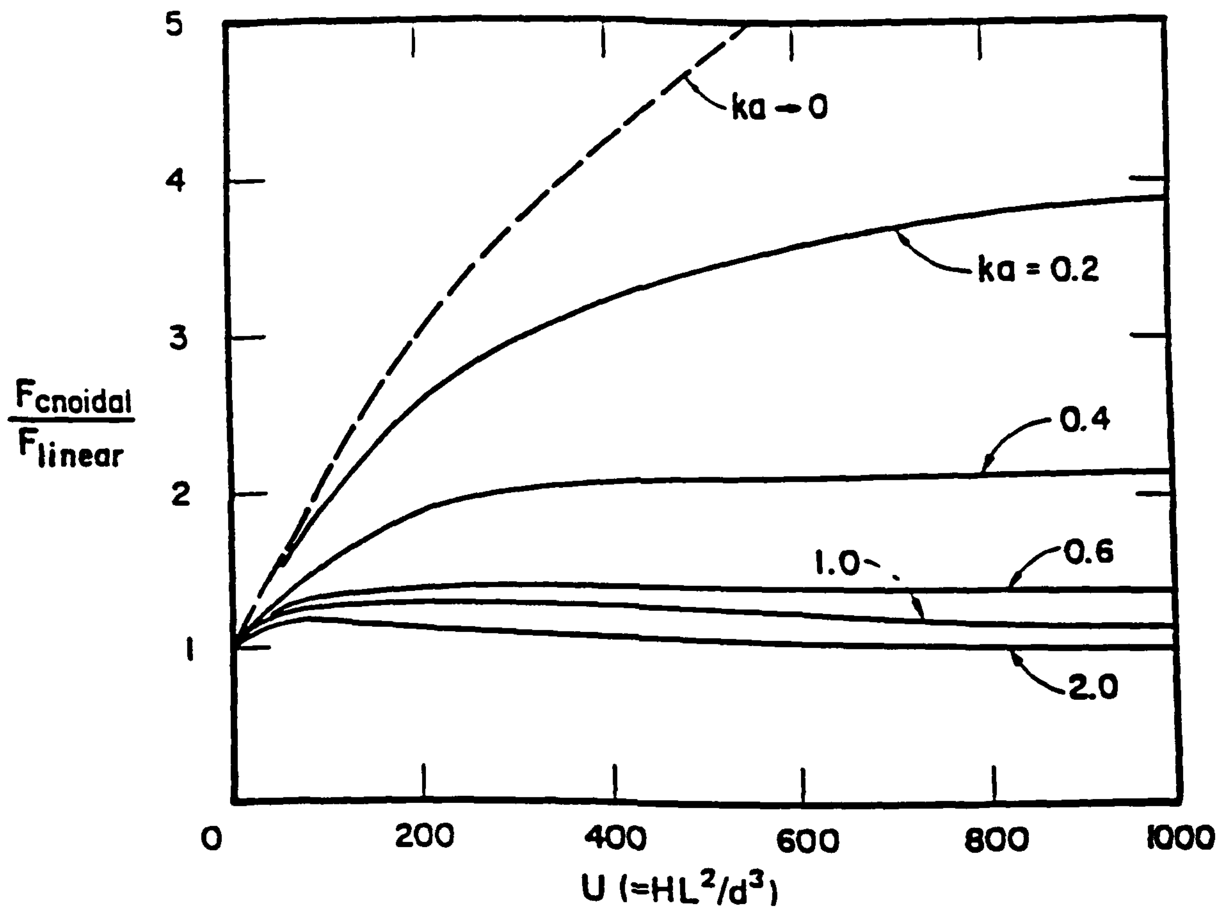


Figure 10
Nonlinear shallow wave forces on a vertical circular cylinder. Ratio of Cnoidal to shallow sinusoidal wave theory force predictions as a function of Ursell number U for various values of ka (from Ref 15).

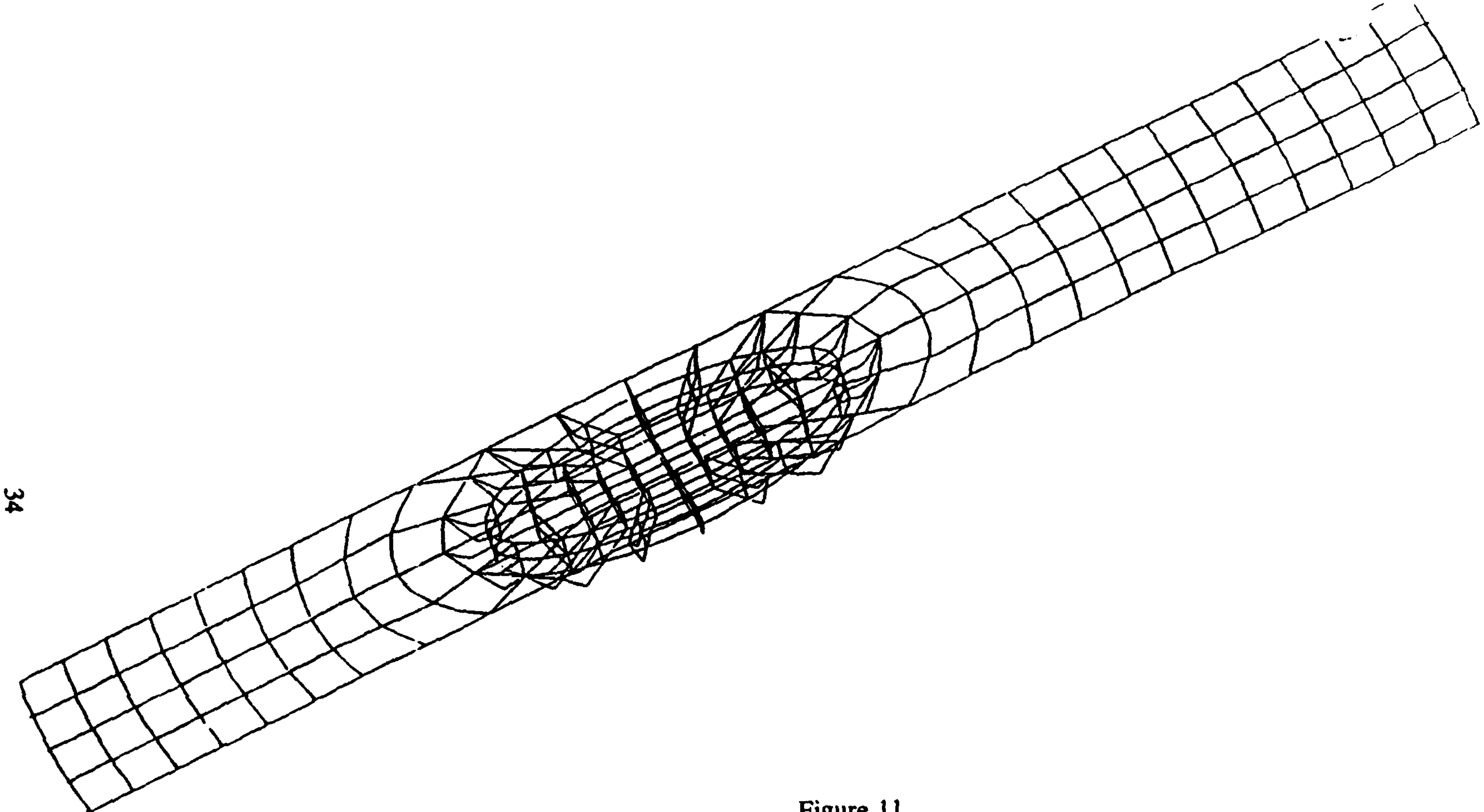

Figure 11
Finite element mesh of the hydraulic model.

## Appendix

## EXTENSION OF BERKHOFF'S WAVE THEORY TO THE SECOND-ORDER WAVE PROBLEMS

### BASIC EQUATIONS

Field equation:

$$\nabla^2 \phi^{(2)} = 0 \tag{A-1}$$

Free surface equation:

$$-\frac{4\omega^2}{g}\phi^{(2)} + \frac{\partial \phi^{(2)}}{\partial z} = \frac{Q}{g}, \qquad z = 0 \tag{A-2}$$

where:

$$Q = -i\,2\,\omega\left[-\left(\nabla \phi^{(1)}\right)^2 + \frac{\phi^{(1)}}{2}\left(\phi^{(1)}_{zz} - \frac{\omega^2}{g}\,\phi^{(1)}_{z}\right)\right]$$

Bottom Condition:

$$\frac{\partial \phi^{(2)}}{\partial x}\frac{\partial h}{\partial x} + \frac{\partial \phi^{(2)}}{\partial y}\frac{\partial h}{\partial y} + \frac{\partial \phi^{(2)}}{\partial z} = 0, \qquad z = -h(x,y) \tag{A-3}$$

The derivation of the reduced equation starts with basic Equations A-1 through A-3 by introducing dimensionless coordinates with the aid of the characteristic length $L = g/\omega^2$ at the free surface and the mean water depth H.

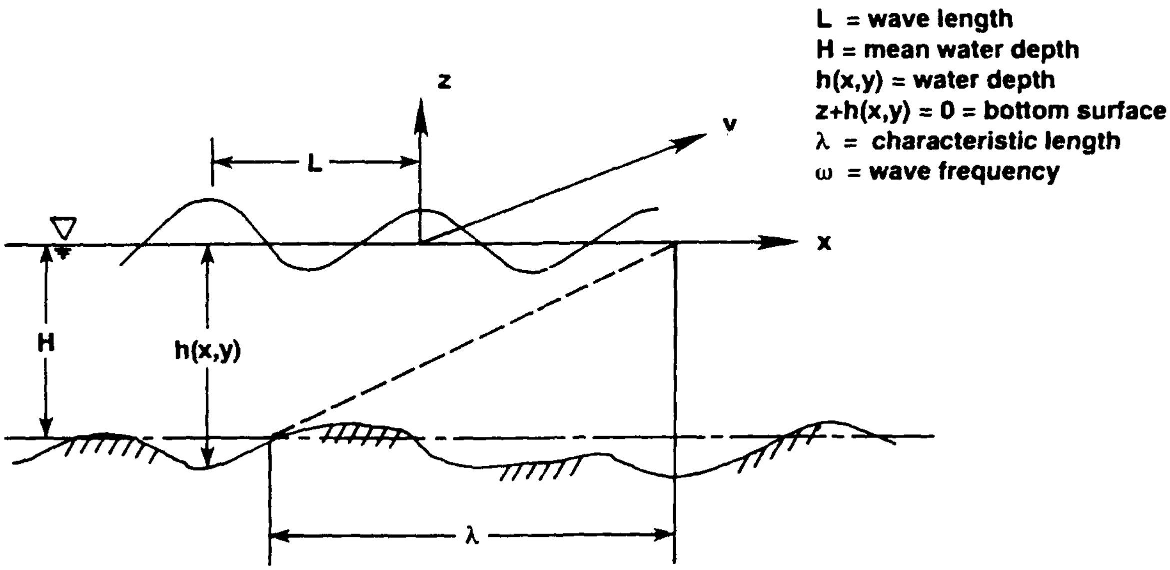


Apply

$$x' = \frac{x}{L} \qquad z' = \frac{z}{H} \qquad \bar{x} = \frac{x}{\lambda}$$

$$y' = \frac{y}{L} \qquad h' = \frac{h}{H} \qquad \bar{y} = \frac{y}{\lambda}$$

and drop the superscript (2). The nondimensional governing equations given in Equations A-1 through A-3 are given as:

$$\frac{\partial^2 \phi}{\partial x'^2} + \frac{\partial^2 \phi}{\partial y'^2} + \left(\frac{L}{H}\right)^2 \frac{\partial^2 \phi}{\partial z'^2} = 0 \tag{A-4}$$

$$\frac{\partial \phi}{\partial z'} - \frac{4\,\omega^2 H}{g}\,\phi = f^*(\phi^{(1)}) = \frac{Q}{g}\,H \tag{A-5}$$

$$\frac{\partial \phi}{\partial z'} + \frac{H^2}{\lambda L}\left(\frac{\partial \phi}{\partial x'}\frac{\partial h'}{\partial \bar{x}} + \frac{\partial \phi_s}{\partial y'}\frac{\partial h'}{\partial \bar{y}}\right) = 0\,, \qquad z = -h' \tag{A-6}$$

Introducing:

$$\mu = \frac{H}{L}, \quad \delta = \frac{\omega^2 H}{g}, \quad \varepsilon = \frac{H}{\sqrt{\lambda L}}$$

Equations A-4 through A-6 can be written as:

$$\frac{\partial^2 \phi}{\partial x'^2} + \frac{\partial^2 \phi}{\partial y'^2} + \frac{1}{\mu^2}\frac{\partial^2 \phi}{\partial z'^2} = 0 \qquad \text{in } \Omega \tag{A-7}$$

$$\frac{\partial \phi}{\partial z'} - 4\,\delta\,\phi = f^*, \qquad z' = 0 \tag{A-8}$$

$$\frac{\partial \phi}{\partial z'} + \varepsilon^2 \left( \frac{\partial \phi}{\partial x'} \frac{\partial h'}{\partial \bar{x}} + \frac{\partial \phi}{\partial y'} \frac{\partial h'}{\partial \bar{y}} \right) = 0, \qquad z' = -h/H = -h' \tag{A-9}$$

Assuming the potential function $\phi$ can be written in the form:

$$\phi(x,y,z) = Z*(h', \mu z')\, \varphi(x', y', \varepsilon z')$$

and developing the function $\varphi$ into a Taylor-series with respect to $\varepsilon z'$:

$$\phi(x,y,z) = Z*(\varphi_o + \varepsilon z' \varphi_1 + \varepsilon^2 z'^2 \varphi_2 + \cdots)$$

Assuming a mild slope:

$$\varepsilon = \sqrt{\frac{H}{\lambda}\,\frac{H}{L}} = \sqrt{\text{slope}} \cdot \sqrt{\frac{H}{L}} << 1$$

Therefore:

$$\phi(x,y,z) = Z(h', \mu z')\, \varphi_o(x', y') \tag{A-10}$$

Substitute Equation A-10 into A-7, and assuming a mild slope ($\varepsilon << 1$), we obtain a simplified equation as

$$Z\left(\frac{\partial^2 \varphi_o}{\partial x'^2} + \frac{\partial^2 \varphi_o}{\partial y'^2}\right) + \frac{\varphi_o}{\mu^2}\frac{\partial^2 Z}{\partial z'^2} = 0$$

That is,

$$\frac{1}{\varphi_o}\left(\frac{\partial^2 \varphi_o}{\partial x'^2} + \frac{\partial^2 \varphi_o}{\partial y'^2}\right) = -\frac{1}{\mu^2 Z}\frac{\partial^2 Z}{\partial z'^2}$$

The left-hand side of the above is a function of (x',y') only, while the right-hand side is a function of z' only. Therefore:

$$\frac{1}{\varphi_o}\left(\frac{\partial^2 \varphi_o}{\partial x'^2} + \frac{\partial^2 \varphi_o}{\partial y'^2}\right) = -4k^2 \qquad \text{(A-11)}$$

and

$$\frac{1}{\mu^2 Z}\frac{\partial^2 Z}{\partial z'^2} = 4k^2, \quad \text{or} \quad \frac{\partial^2 Z}{\partial z'^2} = \mu^2 Z \cdot 4k^2 \qquad \text{(A-12)}$$

Substituting Equation A-10 into A-9:

$$Z\frac{\partial \varphi_o}{\partial z'} + \varepsilon^2(\cdots) = 0, \qquad z' = -h'$$

Therefore:

$$\frac{\partial \varphi_o}{\partial z'} = 0, \qquad z' = -h',\ \varepsilon^2 \to 0 \qquad \text{(A-13)}$$

Substituting Equation A-10 into A-8:

$$\frac{\partial Z}{\partial z'}\varphi_o - 4\delta Z\varphi_o = f^* \quad \text{or} \quad \frac{\partial Z}{\partial z'} - 4\delta Z = f^*/\varphi_o, \qquad z' = 0$$

Therefore, the simplified equations (assuming $\varepsilon << 1$) are given as:

Laplace Equations:

$$\frac{1}{\varphi_o}\left(\frac{\partial^2\varphi_o}{\partial x'^2} + \frac{\partial^2\varphi_o}{\partial y'^2}\right) = -4k^2 \tag{A-14}$$

$$\frac{\partial^2 Z}{\partial z'^2} = \mu^2 Z \cdot 4k^2 \tag{A-15}$$

Free Surface:

$$\frac{\partial Z}{\partial z'} - 4\delta Z = f^*/\varphi_o, \qquad z' = 0 \tag{A-16}$$

Bottom Condition:

$$\frac{\partial Z}{\partial z'} = 0, \qquad z' = -h' \tag{A-17}$$

**Solution of Z**

From Equations A-15 and A-17, the following result can be obtained:

$$Z(h', z') = \frac{\cosh 2k\mu(z' + h')}{\sinh^4(k\mu h')} \tag{A-18}$$

or

$$Z(h,z) = \frac{\cosh 2\left(\frac{k}{L}\right)(z+h)}{\sinh^4\left(\frac{k}{L}\,h\right)}$$

Set k/L = $\kappa$ ... wave number

$$Z(h,z) = \frac{\cosh 2\,\kappa(z+h)}{\sinh^4(\kappa\,h)} \qquad \text{(A-19)}$$

**Solution of $\varphi_o$**

From Laplace Equations A-7 and A-10, we obtained:

$$Z\,\frac{\partial^2\varphi_o}{\partial x'^2} + Z\,\frac{\partial^2\varphi_o}{\partial y'^2} + \frac{\varphi_o}{\mu^2}\,\frac{\partial^2 Z}{\partial z'^2} = 0$$

$$Z\left(\frac{\partial^2\varphi_o}{\partial x'^2} + \frac{\partial^2\varphi_o}{\partial y'^2}\right) + \frac{\varphi_o}{\mu^2}\,\frac{\partial^2 Z}{\partial z'^2} = 0$$

Therefore:

$$\left(\int_{-h'}^{0} Z^2\,dz'\right)\left(\frac{\partial^2\varphi_o}{\partial x'^2} + \frac{\partial^2\varphi_o}{\partial y'^2}\right) + \frac{\varphi_o}{\mu^2}\int_{-h'}^{0} Z(\mu^2 Z \cdot 4\,k^2)\,dz' = 0$$

$$\left(\int_{-h'}^{0} Z^2\,dz'\right)\left(\frac{\partial^2\varphi_o}{\partial x'^2} + \frac{\partial^2\varphi_o}{\partial y'^2}\right) + (4\,k^2\,\varphi_o)\left(\int_{-h'}^{0} Z^2\,dz'\right) = 0 \qquad \text{(A-20)}$$

**Value of $\int_{-h'}^{0} Z^2\,dz'$**

From Equation A-19, the integration of $Z^2$ can be written as:

$$\int_{-h'}^{0} Z^2\,dz' = \int_{-h'}^{0} \frac{\cosh^2(2\,k)\,\mu\,(z'+h')}{\sinh^8(k\,\mu\,h')}\,dz'$$

$$= \frac{1}{2\sinh^8(k\,\mu\,h')} \int_{-h'}^{0} [\cosh 4\,k\,\mu\,(z'+h') + 1]\,dz'$$

$$= \frac{1}{2\sinh^8(k\,\mu\,h')} \left[\frac{1}{4\,k\,\mu} \sinh 4\,k\,\mu\,(z'+h') + 1\right]_{-h'}^{0}$$

$$= \frac{1}{2\sinh^8(k\,\mu\,h')} \left[\frac{\sinh 4\,k\,\mu\,h'}{2(2\,k)\,\mu} + h'\right]$$

$$= \frac{\sinh 4\,k\,\mu\,h'}{4\,k\,\mu\sinh^8(k\,\mu\,h')} \left[\frac{1}{2} + \frac{2(2\,k)\,\mu\,h'}{2\sinh 2(2\,k)\,\mu\,h'}\right]$$

$$= \frac{\sinh 2(2\,k)\,\mu\,h'}{4\,k\,\mu\sinh^8(k\,\mu\,h')} \left[\frac{1}{2} + \frac{2(2\,k)\,\mu\,h'}{2\sinh 2(2\,k)\,\mu\,h'}\right]$$

or

$$\int_{-h'}^{0} Z^2\,dz' = \frac{\sinh 2(2\,\kappa)\,h}{2(2\,\kappa)\,H\sinh^8(\kappa\,h)} \left[\frac{1}{2} + \frac{2(2\,\kappa)\,h}{2\sinh 2(2\,\kappa)\,h}\right]$$

The group velocity, $C_g$, is:

$$C_g = \frac{1}{2}\left[1 + \frac{2\,\kappa\,h}{\sinh(2\,\kappa\,h)}\right]C$$

$$C^2 = \omega^2/\kappa^2$$

Let

$$C_g^{(2)} = \frac{1}{2}\left[1 + \frac{2(2\kappa)h}{\sinh(2(2\kappa)h)}\right]C^{(2)}$$

and

$$[C^{(2)}]^2 = \frac{(2\omega)^2}{(2\kappa)^2}$$

Therefore:

$$\int_{-h'}^{0} Z^2\,dz' = \frac{\sinh 2(2\kappa)h}{2(2\kappa)H\sinh^8(\kappa h)} \cdot \frac{C_g^{(2)}}{C^{(2)}} \qquad \text{(A-21)}$$

From free surface, bottom condition Equation A-16,

$$\frac{\partial Z}{\partial z'} - 4\delta Z = \frac{f^*}{\varphi_o}, \qquad z' = 0$$

$$\frac{\partial Z}{\partial z'} = (2k)\mu\left[\frac{\sinh(2k)\mu(z'+h')}{\sinh^4(k\mu h')}\right]_{z'=0}$$

$$= (2k)\mu\left[\frac{\sinh(2k)\mu h'}{\sinh^4(k\mu h')}\right]$$

Therefore:

$$\frac{\partial Z}{\partial z'} - 4\delta Z = (2k\mu)\frac{\sinh(2k)\mu h'}{\sinh^4(k\mu h')} - 4\delta\frac{\cosh 2k\mu h'}{\sinh^4(k\mu h')}$$

$$= \frac{(2k\mu)\sinh(2k)\mu h' - 4\delta\cosh(2k)\mu h'}{\sinh^4(k\mu h')}$$

$$= \frac{f^*}{\varphi_o}$$

Therefore:

$$\frac{1}{\sinh^4(k\,\mu\,h')} = \frac{f^*}{\varphi_o} \cdot \frac{1}{2\,k\,\mu\,\sinh(2\,k)\,\mu\,h' - 4\,\delta\,\cosh(2\,k)\,\mu\,h'}$$

Therefore:

$$\frac{1}{\sinh^8(k\,\mu\,h')} = \frac{(f^*)^2}{\varphi_o^2} \cdot \frac{1}{[2\,k\,\mu\,\sinh(2\,k)\,\mu\,h' - 4\,\delta\,\cosh(2\,k)\,\mu\,h']^2}$$

or

$$\frac{1}{\sinh^8(\kappa\,h)} = \frac{(f^*)^2}{\varphi_o^2} \cdot \frac{1}{\left[2\,\kappa\,H\,\sinh(2\,\kappa)\,h - \dfrac{4\,\omega^2\,H}{g}\,\cosh(2\,\kappa\,h)\right]^2}$$

Therefore:

$$\int_{-h'}^{0} Z^2\,dz' = \frac{\sinh 2(2\,\kappa)\,h}{2(2\,\kappa)\,H} \cdot \frac{\left[(f^*)^2/\varphi_o^2\right]\left[C_g^{(2)}/C^{(2)}\right]}{\left[2\,\kappa\,H\,\sinh(2\,\kappa)\,h - \dfrac{4\,\omega^2\,H}{g}\,\cosh(2\,\kappa\,h)\right]^2}$$

$$= \frac{F^*_{z=0}}{\varphi_o^2}$$

where:

$$F^* = \frac{\sinh 2(2\,\kappa)\,h}{2(2\,\kappa)\,H} \cdot \frac{(f^*)^2\,C_g^{(2)}/C^{(2)}}{\left[2\,\kappa\,H\,\sinh(2\,\kappa)\,h - \dfrac{4\,\omega^2\,H}{g}\,\cosh(2\,\kappa\,h)\right]^2} \qquad \text{(A-22)}$$

Therefore, Laplace Equation A-20 becomes:

$$\frac{F^*}{\varphi_o^2}\left(\frac{\partial^2 \varphi_o}{\partial x^2} + \frac{\partial^2 \varphi_o}{\partial y^2}\right) \cdot L^2 + 4 k^2 \varphi_o \cdot \frac{f^*}{\varphi_o^2} = 0$$

Since $\varphi_o \neq 0$,

$$\frac{\partial}{\partial x}\left(F^* \frac{\partial \varphi_o}{\partial x}\right) + \frac{\partial}{\partial y}\left(F^* \frac{\partial \varphi_o}{\partial y}\right) + 4 k^2 F^* \varphi_o = 0 \qquad \text{(A-23)}$$

Equation A-23 is the reduced diffraction-refraction equation.

## DISTRIBUTION LIST

ARMY / HQDA (DAEN-ZCM), WASHINGTON, DC
CNA / TECH LIB, ALEXANDRIA, VA
CNO / DCNO, LOGS, OP-0424C, WASHINGTON, DC
COMNAVBEACHGRU TWO / CO, NORFOLK, VA
NAVFACENGCOM / CO, ALEXANDRIA, VA
NAVFACENGCOM / CODE 03T, ALEXANDRIA, VA
NAVFACENGCOM / CODE 04A3C, ALEXANDRIA, VA
NAVFACENGCOM / CODE 06, ALEXANDRIA, VA
NSWC / CODE 1235, BETHESDA, MD
ONT / CODE 226, ARLINGTON, VA

## DISTRIBUTION QUESTIONNAIRE

**The Naval Civil Engineering Laboratory is revising its primary distribution lists.**

**SUBJECT CATEGORIES**

1 **SHORE FACILITIES**
1A Construction methods and materials (including corrosion control, coatings)
1B Waterfront structures (maintenance/deterioration control)
1C Utilities (including power conditioning)
1D Explosives safety
1E Aviation Engineering Test Facilities
1F Fire prevention and control
1G Antenna technology
1H Structural analysis and design (including numerical and computer techniques)
1J Protective construction (including hardened shelters, shock and vibration studies)
1K Soil/rock mechanics
1L Airfields and pavements
1M Physical security
2 **ADVANCED BASE AND AMPHIBIOUS FACILITIES**
2A Base facilities (including shelters, power generation, water supplies)
2B Expedient roads/airfields/bridges
2C Over-the-beach operations (including breakwaters, wave forces)
2D POL storage, transfer, and distribution
2E Polar engineering
3 **ENERGY/POWER GENERATION**
3A Thermal conservation (thermal engineering of buildings, HVAC systems, energy loss measurement, power generation)
3B Controls and electrical conservation (electrical systems, energy monitoring and control systems)
3C Fuel flexibility (liquid fuels, coal utilization, energy from solid waste)
3D Alternate energy source (geothermal power, photovoltaic power systems, solar systems, wind systems, energy storage systems)
3E Site data and systems integration (energy resource data, integrating energy systems)
3F EMCS design
4 **ENVIRONMENTAL PROTECTION**
4A Solid waste management
4B Hazardous/toxic materials management
4C Waterwaste management and sanitary engineering
4D Oil pollution removal and recovery
4E Air pollution
4F Noise abatement
5 **OCEAN ENGINEERING**
5A Seafloor soils and foundations
5B Seafloor construction systems and operations (including diver and manipulator tools)
5C Undersea structures and materials
5D Anchors and moorings
5E Undersea power systems, electromechanical cables, and connectors
5F Pressure vessel facilities
5G Physical environment (including site surveying)
5H Ocean-based concrete structures
5J Hyperbaric chambers
5K Undersea cable dynamics
**ARMY FEAP**
BDG Shore Facilities
NRG Energy
ENV Environmental/Natural Responses
MGT Management
PRR Pavements/Railroads

**TYPES OF DOCUMENTS**

**D** – Techdata Sheets; **R** – Technical Reports and Technical Notes; **G** – NCEL Guides and Abstracts; **I** – Index to TDS; **U** – User Guides; ☐ None - remove my name

Old Address: ______________________________
______________________________
______________________________
______________________________

Telephone No.: ______________________________

New Address: ______________________________
______________________________
______________________________
______________________________

Telephone No.: ______________________________

## INSTRUCTIONS

The Naval Civil Engineering Laboratory has revised its primary distribution lists. To help us verify our records and update our data base, please do the following:

- Add - circle number on list
- Remove my name from all your lists - check box on list.
- Change my address - line out incorrect line and write in correction **(DO NOT REMOVE LABEL).**
- Number of copies should be entered after the title of the subject categories you select.
- Are we sending you the correct type of document? If not, circle the type(s) of document(s) you want to receive listed on the back of this card.

Fold on line, staple, and drop in mail.

---

**DEPARTMENT OF THE NAVY**
Naval Civil Engineering Laboratory
560 Laboratory Drive
Port Hueneme CA 93043-4328

Official Business
Penalty for Private Use, $300

NO POSTAGE NECESSARY IF MAILED IN THE UNITED STATES

**BUSINESS REPLY CARD**
FIRST CLASS PERMIT NO. 12503 WASH D.C.

POSTAGE WILL BE PAID BY ADDRESSEE

**COMMANDING OFFICER**
**CODE L34**
**560 LABORATORY DRIVE**
**NAVAL CIVIL ENGINEERING LABORATORY**
**PORT HUENEME CA 93043-4328**

# NCEL DOCUMENT EVALUATION

You are number one with us; how do we rate with you?

We at NCEL want to provide you our customer the best possible reports but we need your help. Therefore, I ask you to please take the time from your busy schedule to fill out this questionnaire. Your response will assist us in providing the best reports possible for our users. I wish to thank you in advance for your assistance. I assure you that the information you provide will help us to be more responsive to your future needs.

RNStorer

R. N. STORER, Ph.D, P.E.
Technical Director

---

DOCUMENT NO. ________ TITLE OF DOCUMENT: ________________________

________________________

---

Date: ________ Respondent Organization : ________________________

Name: ________________________ Activity Code: ________________

Phone: ________________________ Grade/Rank: ________________

Category (*please check*):

Sponsor _____ User _____ Proponent _____ Other (*Specify*) ________________

Please answer on your behalf only; not on your organization's. Please check (*use an X*) only the block that most closely describes your attitude or feeling toward that statement:

SA Strongly Agree A Agree O Neutral D Disagree SD Strongly Disagree

---

| | SA | A | N | D | SD |
|---|---|---|---|---|---|
| 1. The technical quality of the report is comparable to most of my other sources of technical information. | ( ) | ( ) | ( ) | ( ) | ( ) |
| 2. The report will make significant improvements in the cost and or performance of my operation. | ( ) | ( ) | ( ) | ( ) | ( ) |
| 3. The report acknowledges related work accomplished by others. | ( ) | ( ) | ( ) | ( ) | ( ) |
| 4. The report is well formatted. | ( ) | ( ) | ( ) | ( ) | ( ) |
| 5. The report is clearly written. | ( ) | ( ) | ( ) | ( ) | ( ) |
| 6. The conclusions and recommendations are clear and directly supported by the contents of the report. | ( ) | ( ) | ( ) | ( ) | ( ) |
| 7. The graphics, tables, and photographs are well done. | ( ) | ( ) | ( ) | ( ) | ( ) |

| Do you wish to continue getting NCEL reports? | ☐ YES | ☐ NO |
|---|---|---|

Please add any comments (e.g., in what ways can we improve the quality of our reports?) on the back of this form.

**Comments:**

Fold on line, staple, and drop in mail.


**DEPARTMENT OF THE NAVY**
Naval Civil Engineering Laboratory
560 Laboratory Drive
Port Hueneme CA 93043-4328


Official Business
Penalty for Private Use, $300

NO POSTAGE NECESSARY IF MAILED IN THE UNITED STATES

**BUSINESS REPLY CARD**
FIRST CLASS PERMIT NO. 12503 WASH D.C.

POSTAGE WILL BE PAID BY ADDRESSEE

**COMMANDING OFFICER**
**CODE L03**
**560 LABORATORY DRIVE**
**NAVAL CIVIL ENGINEERING LABORATORY**
**PORT HUENEME CA 93043-4328**